Transfer of water and contaminants in the Chalk unsaturated zone – underground quarry of Saint-Martin-le-Nœud

Danièle Valdes, Ningxin Chen, Marc Dumont, Christelle Marlin, Hélène Blanchoud, Roger Guérin, Julien Guillemoteau, Fabrice Alliot, Romane Nespoulet, Emmanuel Aubry, et al.

Transfer of water and contaminants in the Chalk unsaturated zone – underground quarry of Saint-Martin-le-Nœud

Danièle Valdes[1]*, Ningxin Chen[1], Marc Dumont[1], Christelle Marlin[2], Hélène Blanchoud[1,3], Roger Guérin[1], Julien Guillemoteau[4], Fabrice Alliot[1], Romane Nespoulet[1], Emmanuel Aubry[1], Maryse Rouelle[1], Cyrille Fauchard[5], Philippe Gombert[6] and Pierre Ribstein[1]

[1]Sorbonne Université, CNRS, EPHE, UMR 7619 METIS, F-75005 Paris, France

[2]UMR 8148 GEOPS, Université Saclay, CNRS bâtiment 504, 91405 Orsay, France

[3]EPHE, PSL Research University, UMR METIS 7619 (SU, CNRS, EPHE), 4 rue Jussieu, F-75005 Paris, France

[4]Universität Potsdam, Institut für Geowissenschaften, 14476 Potsdam-Golm, Germany

[5]CEREMA, Equipe Recherche ENDSUM, Direction Territoriale Normandie Centre, Le Grand-Quevilly, France

[6]Institut National de l'Environnement Industriel et des Risques (INERIS), 60550 Verneuil-en-Halatte, France

DV, 0000-0003-2843-4065; MD, 0000-0002-1629-511X; RG, 0000-0001-7758-6984; JG, 0000-0003-3807-5609; FA, 0000-0002-1335-1294; RN, 0000-0002-9066-8463; CF, 0000-0002-9756-6179; PR, 0000-0002-1710-8267

*Correspondence: daniele.valdes_lao@upmc.fr

Abstract: The aim of this study is to understand the water and contaminant (nitrate and atrazine) transfer in the unsaturated zone (UZ) of Chalk. For this, the underground quarry of Saint-Martin-le-Nœud is an exceptional site because it permits entry to the aquifer at the limit between the UZ and the saturated zone (SZ). It provides direct access to the water table: underground lakes and the output of the UZ (percolation water at the ceiling). The thicknesses of the UZ and the clay-with-flints (CwF) layer that overlie the Chalk, vary along the 1200 m length of the quarry.

From 2012, the chemical evolution and the flow variability of groundwater are characterized for 16 sites with different UZ properties. Chalk groundwater has highly spatially variable hydrodynamic behaviour and geochemical properties. A peak of contaminants is observed in the UZ around 15–20 m depth, with differing behaviours of nitrate and atrazine. The downward matrix water velocity is estimated to be from 0.3 to over 0.72 m a^{-1}, and the water table is mainly composed of 'old' water resulting from transfer through the matrix. A thick CwF layer modifies (1) the transfer processes: surface water is stored in a sort of 'near-surface perched groundwater', the infiltration is concentrated by preferential pathways; and (2) water quality: pesticides degradation processes occur in the perched groundwater.

The Chalk aquifer is a major resource for water supply in France, Belgium, England, Germany and The Netherlands (Lapworth *et al.* 2015). In France, where the Chalk of the Paris Basin covers an area of approximately 110 000 km^2, the aquifer provides close to 12 billion m^3 a^{-1} of water (Lallahem 2002). For several decades, this resource has been threatened by high anthropogenic pressure in the form of intensive agriculture using fertilizers and pesticides, which have caused degradation of the groundwater quality (Brouyère *et al.* 2004; Baran *et al.* 2008; Orban *et al.* 2010). The contamination of drinking water by nitrate and atrazine is recognized as a crucial issue for human health (Comly 1945; Espejo-Herrera *et al.* 2016).

In the Paris Basin, despite a reduction in the use of nitrates and a ban on atrazine in France in 2003, their concentrations in Chalk groundwater can exceed the authorized French standards for drinking water production of 50 mg l^{-1} and 0.1 µg l^{-1} for each individual pesticide (El Gaouzi *et al.* 2013), while the concentration of nitrate in the unconfined Chalk aquifer is increasing over the majority of the territory. The temporal trend of nitrate content between 2010 and 2017 was positive for 83% of the Paris Basin area with 47% having a trend higher

From: Farrell, R. P., Massei, N., Foley, A. E., Howlett, P. R. and West, L. J. (eds) *The Chalk Aquifers of Northern Europe*. Geological Society, London, Special Publications, **517**, https://doi.org/10.1144/SP517-2020-231

than 0.25 mg l^{-1} a^{-1} (Public data from the French 'Ministère de la Transition Ecologique').

Most studies of Chalk groundwater deal with the hydrogeochemical responses at the outlets of the aquifer: the springs (natural outlet) or the wells (anthropic outlet) (Kloppmann *et al.* 1994; Valdes *et al.* 2005, 2006; Stuart and Smedley 2009; Orban *et al.* 2010; Ascott *et al.* 2016; Cao *et al.* 2020). The observations made in these studies concern processes both in the saturated zone (SZ) and the unsaturated zone (UZ), and it is difficult to separate them in order to understand specifically the processes occurring only in the UZ of the Chalk aquifers.

The underground quarry of Saint-Martin-le-Nœud (Fig. 1) is an exceptional site for studying the transfer of water and contaminants in the UZ of Chalk. It permits entry to the aquifer to analyse directly the chemical evolution and the flow variability of groundwater as it reaches the water table.

This underground quarry was dug in Chalk at the limit between the UZ and the SZ and is located in the Upper Cretaceous Chalk layer of the Paris Basin. The water table is intercepted in the deeper parts of the quarry, in the form of underground lakes. The water percolating at the ceiling of the quarry is interstitial solution circulating through the UZ. This set-up gives direct access to the water at the base of the UZ and the top of the SZ, and the behaviour of both compartments can therefore be studied. The quarry is dug to a maximum depth of 31 m and a layer of clay-with-flints (CwF) of varying thickness covers the Chalk. The surface is used as agricultural land on which nitrate fertilizers have been applied since the 1950s and atrazine pesticides from 1977 to 2003.

The first hydrogeological investigations in the quarry started in 2012 with measurements of the underground lakes and percolating water along the quarry, including: time series of percolating flow, lake water levels, temperature and electrical conductivity, as well as discrete measurements of major ions, pesticide concentrations and tritium

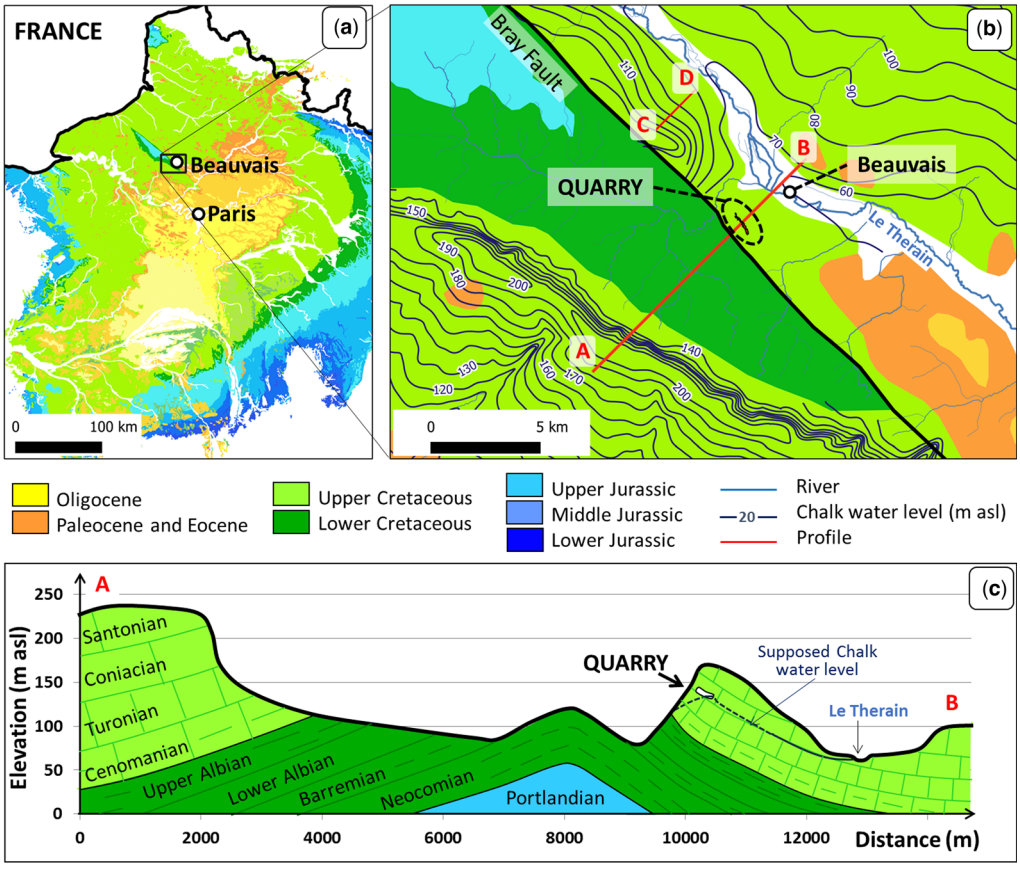

Fig. 1. (**a**) Geological map of the Paris Basin; (**b**) geological map around the Bray anticline; (**c**) sketch of the geological section of the Bray anticline with the location of the quarry and the supposed Chalk water level.

content (Barhoum 2014; Barhoum *et al.* 2014; Chen 2019; Chen *et al.* 2019*a*, *b*).

The long-term study of Saint-Martin-le-Nœud provides a better understanding of and new insights into the Chalk transfer processes into the UZ, mainly those concerning water and contaminant transfer. Insight has been obtained into the following:

(1) *The local variability in groundwater chemistry upon reaching the water table*. Spatial and temporal heterogeneities of Chalk groundwater chemistry have been widely studied. The chemical variability of water is explained by factors such as local variation in rock mineralogy (Edmunds *et al.* 2003; Kloppmann *et al.* 1998) or structural controls (Valdes *et al.* 2007), and human pollution especially due to agricultural activities (Kloppmann *et al.* 1994; Hakoun *et al.* 2017), as well as mixing between waters of different residence times and origins including rapid fissure water and matrix water (Gillon *et al.* 2010). However, most of the studies are performed at large scale (not local scale) and typically concern concentrations beneath the water table, rather than at the point at which UZ groundwater reaches the water table.

(2) *The balance of fracture v. matrix flow*. The Chalk is a complex carbonate rock with double porosity: matrix and fractures – eventually a triple porosity in karst areas with the presence of conduits (Barker and Foster 1981). The matrix is characterized by a low permeability of approximately 10^{-8} m s^{-1} and a high total porosity from 20 to 40%, while the fractures are characterized by a higher permeability in the range of 10^{-5}–10^{-6} m s^{-1} (Megnien 1978; Bloomfield 1996) and a low porosity of less than 1%. Water transfer processes occur in both the matrix and fractures. A two-way transfer process of water and contaminants characterizes the Chalk aquifer: 'piston flow' (transfer of energy only: the old water is displaced by a new input of water) and 'direct transfer' (transfer of water) occurring within fractures and fissures. The water velocity is much lower in the piston-flow case than in the direct-transfer case. The transfer processes and the proportions and exchanges between the matrix and fissures have been widely studied but remain difficult to define. Most studies consider that the transfer mainly occurs through the matrix (Mathias *et al.* 2005; Cooper *et al.* 2006). The transfer through fractures may be active under specific conditions, such as high rainfall intensity and high soil moisture (Haria *et al.* 2003; Ireson *et al.* 2009; Ireson and Butler 2011).

(3) *The transport of contaminants*. Some models have been developed to simulate nitrate and atrazine transfer in the Chalk aquifer (Brouyère 2006; Gutierrez and Baran 2009; Orban *et al.* 2010; Smith *et al.* 2010; Wang *et al.* 2012; Ascott *et al.* 2016), but the lack of knowledge of the processes occurring in the UZ remains a limitation. A few studies have directly observed nitrate profiles in the Chalk UZ, obtaining transfer velocities of the order of 0.5–1 m a^{-1}, and therefore estimating the arrival of nitrates in the water table in the next few years, at most a few decades (Foster *et al.* 1982; Gutierrez and Baran 2009; Surdyk *et al.* 2021). Atrazine is more complex to study because of its susceptibility to degradation and sorption processes. This contaminant moves with the water by advection but can be affected, mainly in the UZ, by several other processes depending on its physico-chemical and soil properties (Chefetz *et al.* 2004). Moreover, due to degradation processes, the main degradation product of atrazine, deethylatrazine (DEA), was the most frequently detected substance in Chalk groundwater of the Paris Basin over the period 2012–17 (AESN 2020). According to Issa and Wood (1999) and Johnson *et al.* (2000), the degradation processes mainly occur in the soil, but they could also occur in the UZ at a lower rate. The need for improved knowledge on the contaminant transport processes is a major issue in hydrogeology.

(4) *The role of the clay-with-flints cover on the water and contaminant transfer in the Chalk aquifer*. The CwF results primarily from the weathering of Chalk (Laignel *et al.* 1999). It may be thick (up to 40 m in Upper Normandy) or thinner (a few metres) and even absent in the Paris Basin (Valdes *et al.* 2014). In the past, this layer was considered to be impervious. Later, Klinck *et al.* (1998) measured *in situ* the hydraulic conductivity of CwF and found greatly variable values that may be high locally: from 10^{-4} to 10^{-9} m s^{-1}. Using self-potential measurements, Jardani *et al.* (2006) provided evidence of preferential pathways and storage zones in CwF and showed the presence of sinkholes and cryptosinkholes, which cause much higher permeability than that of classic clays. At the regional scale of Upper Normandy, Valdes *et al.* (2014) showed a thick CwF layer above karstic Chalk, which may lead to perched groundwater and local infiltration via developed karst inducing locally preferential pathways with concentrated infiltration, while in the case of a thin CwF layer, the infiltration is more diffuse.

This paper presents the main results of the study of the Saint-Martin-le-Nœud quarry over almost a decade (2012 to 2020). It is a synthesis of previously published work (Barhoum 2014; Barhoum *et al.* 2014; Chen 2019; Chen *et al.* 2019*a*, *b*) but also of new results that have not yet been published. First, the characterization of the site is presented in detail: (1) a description of the variability of the UZ characteristics; (2) a description of the groundwater characteristics in both the SZ and UZ: spatial and temporal variation of the groundwater quality (especially atrazine and nitrate) and of the groundwater flow; and (3) a cross-analysis of the chemical and hydrodynamic characteristics of the groundwater and UZ characteristics. New insights into the processes of water and contaminant transfer in the Chalk UZ and the impact of the CwF layers on it are then discussed.

Site characterization

General settings of Saint-Martin-le-Nœud underground quarry

The Saint-Martin-le-Nœud underground Chalk quarry belongs to the French National Observatory Service of Karst – (namely, SNO Karst; Jourde *et al.* 2018), part of the national research infrastructure eLTER-France OZCAR (the French network of Critical Zone Observatories; Gaillardet *et al.* 2018). It is located in the Haut-de-France region in the northern part of the Paris Basin (5 km south of Beauvais, 70 km north of Paris, Fig. 1). The quarry was exploited for Chalk blocks by the room-and-pillar method from the twelfth to the eighteenth centuries, and is made up of corridors, galleries and rooms. It is about 1200 m long and 150 m wide (Fig. 2).

Geology and hydrogeology. The quarry belongs to the eastern part of the Bray anticline where the Chalk strata dip approximately 12° NNE (Fig. 1b, c). It was dug into the Upper Cretaceous Chalk layer dating from the Coniacian and Turonian (Fig. 1c). In this study area, the Chalk aquifer may be considered as a double-porosity aquifer with matrix and fractures, as field observations give no evidence of karst conduits, only minimal dissolution in some fractures. The total porosity of the Chalk in the quarry has been measured as approximately 40% (Lafrance 2016), the fracture porosity is estimated at around 1% (Megnien 1978). A layer of CwF covers the quarry Chalk with a variable thickness from nearly 0 to about 10 m (Barhoum *et al.* 2014).

At a depth of 18–31 m (Barhoum 2014), the quarry gives direct access to the limit between the UZ and the SZ. The lowest parts of the cavity lie at the water table, forming a series of underground lakes and water percolates at the ceiling of the quarry. The study focuses on 16 sites: the lake and associated percolation areas (Fig. 2). The list of the sites (name and three-letter site code) is given in Table 1.

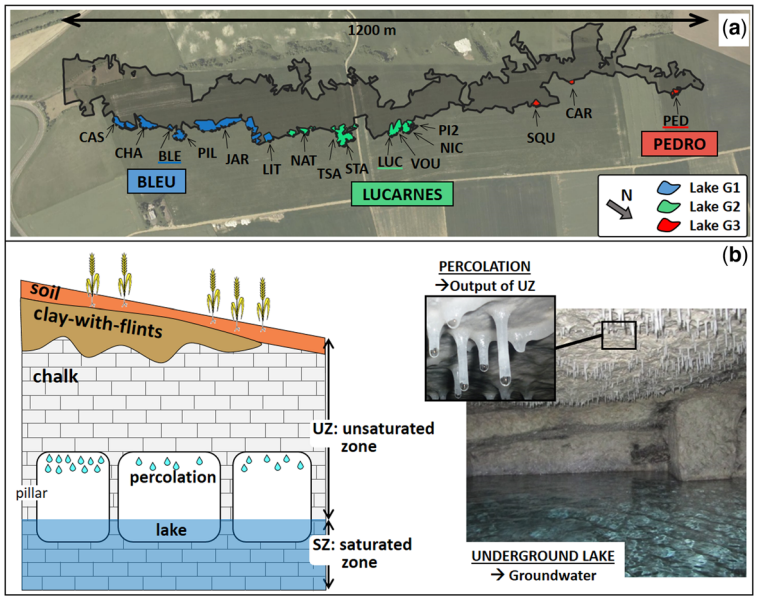

Fig. 2. (**a**) Map of the quarry and location of the underground lakes. (**b**) Cross-section of the quarry from the surface to the SZ of Chalk (with rooms and pillars) and photos of percolating water and underground lakes with stalactites on the ceiling.

Table 1. *Study site characteristics: UZ thickness, bulk soil conductivity from electromagnetic induction measurements as a proxy of clay thickness and group*

Site name	Code	UZ thickness (m)	Electrical conductivity (mS m^{-1})	Group
Casteret	CAS	29.1	30.0	1
Champignonnières	CHA	29.5	36.1	1
Bleu	BLE	29.7	47.5	1
Piliers	PIL	29.8	44.0	1
Jardin	JAR	29.5	59.0	1
Lithoclase	LIT	31.0	56.4	1
Nation	NAT	31.0	71.0	2
Tsar	TSA	31.0	72.0	2
Stalactites	STA	29.2	72.0	2
Lucarnes	LUC	27.3	71.0	2
Voutes	VOU	27.3	72.0	2
Niches	NIC	26.0	70.0	2
Piliers2	PI2	24.2	70.0	2
Squelettes	SQU	24.0	43.5	3
Carrefour	CAR	18.0	28.0	3
Pedro	PED	21.6	20.0	3

From Chen (2019).

The percolating water comes directly from the UZ and flows from the ceiling of the lowest parts of the quarry, most often above the lakes, and forms 4–5 cm-long stalactites. Percolation is variable in time and space. This percolating water is spatially and temporally variable and may be permanent throughout the year in some places (Barhoum *et al.* 2014).

The quarry is located under a topographic ridge along a SSE/NNW axis, which is the major axis of the anticline (Fig. 1b, c). The underground lakes are aligned in low-lying areas, along the same orientation. The lake water levels correspond to the Chalk piezometric levels given by the hydrogeological map of Beauvais (BRGM 1969), and their temporal variability is very similar to that of the Chalk water table recorded in Beauvais (data exported from the public website 'Portail ADES' http://www.ades.eaufrance.fr/). The piezometric map of the Chalk (data provided by SIGES, BRGM) is shown in Figure 1b. Due to the absence of observation wells, there is no piezometric information in the proximity of the quarry. However, the piezometric map indicates that the water table is drained to the NE by the Thérain River. Furthermore, studies injecting dye tracer carried out in 2010 (INERIS 2010) and recently in 2021 in the underground lakes have shown that the lakes also flow toward the Thérain River and no water exchange was observed between the lakes. A cross-section of the piezometric level is proposed in Figure 1c. Between the quarry and the Thérain River, the hydraulic gradient is rather high (about 2.5%), which is quite coherent with the hydraulic gradient of approximately 2% computed along the C–D profile in a small topographic dome similar to that of the quarry (Fig. 1b). In the SW of the quarry, the piezometric gradient is unknown. Transposition of the piezometry of the area around the C–D profile to the quarry area allows us to propose a flow toward the anticline. Thus, the underground lakes are probably on or near the piezometric ridge and are supplied almost exclusively by groundwater flowing vertically through the UZ. The lake waters are therefore assumed to result from a mixture of percolating water dripping from the ceiling of the quarry or water passing directly through the chalky pillars and the walls in the quarry to the water table.

Climate and land use. The climate is oceanic, with an average annual temperature of 11°C and an average annual rainfall of 700 mm (data from 1981 to 2010 provided by Météo-France at the Beauvais station). The evapotranspiration ranges from 450 to 500 mm a^{-1} (Chen 2019).

The soil has been cultivated (corn, wheat and rape) since at least 1950. The agricultural practices (type of cultivation, fertilizers, and pesticide inputs) since the 1970s are known thanks to the farmer and owner of the field who recorded all this information in a notebook. In the field above the quarry, atrazine was used from 1977 to 2003 and nitrogen fertilizers have been widely used in the area since the 1950s (Le Noë *et al.* 2017).

Characterization of unsaturated zone

Geophysical measurements. Firstly, the UZ thickness was determined with an underground GPS

survey in 2012 (Barhoum *et al.* 2014). Secondly, the CwF layer was characterized using geophysical measurements at the surface above the quarry. Electrical or electromagnetic methods energize the subsurface in order to estimate electrical conductivity or its inverse, electrical resistivity. CwF thickness is related to this conductivity because of the electrical properties of clay and water. The electrical conductivity of the soil can be used as a proxy for the CwF layer thickness (Barhoum *et al.* 2014). The higher the electrical conductivity (or the lower the electrical resistivity), the greater the thickness of the CwF.

Electromagnetic induction (EMI) allows one to map near-surface electrical variation over the entire quarry (McNeill 1980). Two geophysical surveys were carried out: in September 2013 using an EM31 (Barhoum *et al.* 2014) and in May 2019 using a CMD explorer.

Two-dimensional (2D) electrical resistivity tomography (ERT) is a direct current electrical method investigating the distribution of lateral and vertical electrical resistivity (Griffiths and Barker 1993). It can provide deep 2D imaging of the bulk resistivity (Daily and Owen 1991). The ERT profiles were carried out using a SyscalPro resistivity meter in May 2019.

Characterization of UZ thickness and CwF layer. The EMI map (Fig. 3a) shows a large spatial variability of the surface apparent electrical conductivity with values ranging from 1 to 70 mS m^{-1} (from 1000 to 14.3 Ω m in terms of apparent electrical resistivity). The most conductive areas correspond to higher clay content in the soil and thus wetter subsurface. On the other hand, the less conductive areas are interpreted as having a thinner surface layer of CwF (eventually no clay). The electrical conductivity was determined for each of the 16 sites of the quarry (Table 1).

According to the differences in UZ characteristics, CwF thickness and UZ thickness (Table 1), the quarry can be divided into three areas and the sites separated into three groups:

- Group 1 (G1): CAS, CHA, BLE, PIL, JAR and LIT. These sites have the highest UZ thickness (around 30 m) with a thin layer of CwF.
- Group 2 (G2): NAT, TSA, STA, LUC, VOU, NIC and PI2. These sites have a high UZ thickness (around 28 m) with a thick layer of CwF.
- Group 3 (G3): SQU, CAR and PED. These sites have the lowest UZ thickness (around 20 m) with a thin layer of CwF.

The two electrical profiles carried out on the surface above the Group 1 lakes (P1 in Fig. 3a, b) and Group 2 lakes (P2 in Fig. 3a, b) are different, giving evidence of different subsurface geometries. The resistivity of the P1 profile was generally higher than that of P2. The areas of lower resistivity (<40 Ω

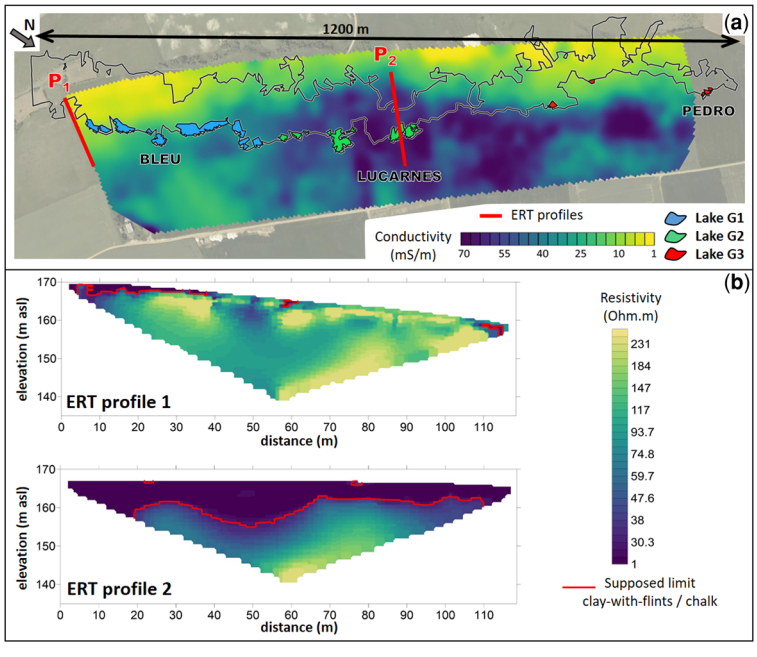

Fig. 3. (**a**) EMI bulk conductivity map from 0 to 4.2 m depth. (**b**) ERT: Electrical resistivity profiles (May 2019).

m) are interpreted as areas covered by a surface CwF layer. Thus, in profile P1, a thin CwF layer (max. 2–3 m) is only present in the northern part. In profile P2, the CwF layer is continuous and thick (max. 10 m). Its geometry shows clay-filled depressions, as already reported by Jardani *et al.* (2006).

Groundwater characterization

Data collection

Sampling and measurements. Measurements and sampling of the percolating water and the underground lakes of the 16 sites were performed. The study of the lakes began in 2012 and that of the percolating waters during 2014–15. Field campaigns were conducted approximately every 2 months from 2012 to 2020.

The 16 lakes were sampled and electrical conductivity, temperature and water level were measured *in situ*. In several lakes, time series of the water level, electrical conductivity and temperature were recorded using CTD (conductivity, temperature, depth)-Diver probes.

Sampling from each of the 16 percolation sites was achieved using 250 ml beakers installed under the quarry ceiling. Percolating volume, electrical conductivity and temperature were measured *in situ*. In several sites, time series of percolating flow were recorded using rain gauges. Due to technical problems and equipment failure, the time series may have gaps in the records.

From April 2016 to September 2017, seven complete campaigns were carried out: 12 April 2016, 6 June 2016, 23 June 2016, 5 September 2016, 9 January 2017, 27 February 2017 and 5 September 2017. The dataset 'April 2016–September 2017' is composed of 94 samples for the lakes and 97 for the percolating water for the 16 sites. Data are available on the water level of the lakes, percolating flow, and geochemical analysis of major ions (including nitrate) and pesticides for both lakes and percolating waters.

Geochemical analysis. Major ions (Ca^{2+}, K^{+}, Na^{+}, Mg^{2+}, NO_3^-, Cl^-, SO_4^{2-}) were analysed using ion chromatography (Dionex ISC 3000). The accuracy is 1 mg l^{-1} with 5% uncertainty. These analyses were performed for all samples. Alkalinity (HCO_3^-) was measured by acid titration. It was performed for all lake samples and for about half of the percolation samples. Calcite precipitation was observed in some of the beakers sampling the percolation water, and alkalinity was not measured for these samples. When alkalinity was available, the ionic balance was calculated.

Atrazine and its metabolite deethylatrazine (DEA) were analysed through solid phase extraction LC-MS/MS (liquid chromatography mass spectrometry) (Agilent Technology) using only 2 ml water samples (Blanchoud *et al.* 2020). The quantification limit was 20 ng l^{-1} with 20% uncertainty. These analyses were performed on lake and percolating water, in April 2013 at the Bleu and Pedro sites only, from April 2016 to September 2017 at all 16 sites, and thereafter only at eight selected sites including Bleu, Lucarnes and Pedro. The atrazine degradation ratio (DAR) is defined as DAR = [DEA]/[Atrazine]. It is an indicator of the atrazine degradation processes. The higher the DAR, the greater the degradation processes.

The tritium content in groundwater may be used to estimate the residence time of the water. It was determined using the electrolytic enrichment and liquid scintillation counting methods with a standard deviation measured for each sample (Thatcher *et al.* 1977) at the University of Avignon Emmah Laboratory. Tritium analyses were performed for ten sites including Bleu, Lucarnes and Pedro for the percolation water in April 2016 and for the lakes in March 2016. The tritium content in groundwater may be used to estimate the age of the water using piston flow models (Maloszewski and Zuber 1996; Chen *et al.* 2019*a*).

Groundwater results. The geochemical and hydrodynamic data collected for groundwater (lakes and percolating water) are presented; first, the spatial approach, for the 16 sites based on 2016–17 data, and second, the temporal approach, on the longest time series, i.e. 2012–20, for three sites, one per group: Bleu for Group 1, Lucarnes for Group 2 and Pedro for Group 3 (Figs 2 & 3, Table 1).

Spatial approach. The data concern both percolation water and underground lakes. The spatial variation of water quality as well as of the hydrodynamics of percolating water has already been presented and discussed by Chen *et al.* (2019*a*).

The main statistics of the geochemical parameters – mean, minimum, maximum and standard deviation (SD) – for the 16 lakes and the 16 percolation waters of the 'April 2016–September 2017' dataset are shown in Table 2.

The physical and hydrochemical characteristics (normalized lake level – mean centred, electrical conductivity of water, Ca^{2+}, NO_3^-, Cl^-, Mg^{2+}, atrazine, DEA concentrations and the DAR) of groundwater (UZ and SZ) are presented in Figure 4 for the 16 sites along the quarry.

Three main points can be highlighted:

- The percolating water and lake water have different characteristics: the mean electrical conductivity of the percolating water is 483 $\pm$ 159 µS cm^{-1}, while that of the lake water is 554 $\pm$ 77 µS cm^{-1}. At some of the sites, the percolating water is locally more mineralized than the associated lake (e.g. Lucarnes), whereas at other

Table 2. *Principal statistical characteristics of the datasets from the April 2016 to September 2017 campaigns*

	Percolating water				Lake water			
	mean	min	max	SD %	mean	min	max	SD %
Elec. Cond. (µS cm^{-1})	483	249	825	33%	554	276	768	14%
[Ca] (m l^{-1})	79.9	35.0	151.9	38%	95.8	64.7	121.8	17%
[K] (mg l^{-1})	2.4	1.0	11.2	96%	2.4	1.0	9.1	79%
[Na] (mg l^{-1})	8.4	4.1	17.2	37%	9.6	5.4	12.8	25%
[Mg] (mg l^{-1})	2.2	1.0	6.4	51%	2.4	1.2	5.2	33%
[NO_3] (mg l^{-1})	50.5	7.3	144.6	72%	39.8	12.8	94.6	41%
[Cl] (mg l^{-1})	25.3	7.4	58.9	63%	19.5	11.2	41.5	34%
[SO_4] (mg l^{-1})	17.7	2.6	42.3	63%	13.9	8.1	38.5	33%
[Atrazine] (ng l^{-1})	1268	9	15 207	203%	256	25	2420	157%
[DEA] (ng l^{-1})	3643	4	52 120	238%	1257	157	12 050	131%
DAR	3.2	0.05	14.0	67%	5.3	2.0	41.9	95%
Mean				87%				60%

Campaign dates – 2016: 12 April, 6 June, 23 June, 5 September; 2017: 9 January, 27 February, 5 September.
Samples: 94 samples of underground lakes (5--6 depending on the sites), 97 samples of percolating waters (3--7 depending on the sites).

sites the lake water is more mineralized than the percolation water (e.g. Bleu).

- Some water reaches extremely high levels of agricultural contamination, with the highest contamination measured in percolation water. For example, the maximum nitrate concentration in percolating water for Carrefour is 145 mg l^{-1} and the atrazine concentration in Niches is about 15 000 ng l^{-1}.
- Spatially, the geochemical properties of groundwater are different. For percolating water, the electrical conductivity varies from 249 to 825 µS cm^{-1}. For lakes, it varies from 276 to 768 µS cm^{-1}. Even if the range of values is similar between lakes and percolating water, the spatial variability is greater in percolating water than in lakes (the mean SD of all the parameters in Table 2 is 87% for percolating water and 60% for lakes). This spatial variability was observed for all chemical elements. In a more detailed way, the three groups can be characterized as follows.
  - *Group 1, the highest UZ thickness (around 30 m) with a thin layer of CwF*: The annual water level variation of the lakes is 0.60 m on average. The lake water is more mineralized than the percolating water. All chemical species are more concentrated in the lake water than in percolating water. Agricultural water contamination is low in percolation water. In the lakes, average concentrations (mean of all the samples) are 33.8 $\pm$ 4.2 mg l^{-1} of nitrate, 231 $\pm$ 462 ng l^{-1} of atrazine and 1013 $\pm$ 1318 ng l^{-1} of DEA; in the percolating water, average concentrations are 21.2 $\pm$ 10.4 mg l^{-1} of nitrate, 28 $\pm$ 28 ng l^{-1} of atrazine and 58 $\pm$ 95 ng l^{-1} of DEA. Lake Jardin has the highest contamination of Group 1 with a maximum nitrate concentration of 42 mg l^{-1}, a maximum atrazine concentration of 2100 ng l^{-1} and a maximum DEA of 4200 ng l^{-1}. Chloride and magnesium concentrations are low (around 15 and 2 mg l^{-1}, respectively). The DAR of Group 1 is about 3 for lakes and percolation water.
  - *Group 2, a high UZ thickness (approximately 28 m) with a thick layer of CwF*: The annual water level variation of the lakes is 0.43 m on average. Very low variations for Lake Lucarnes and Lake Voutes (0.11 and 0.17 m, respectively, during the 2016–17 period) are observed. All the water in Group 2 is highly contaminated, with a generally higher contamination in the percolation water than in the lakes. In the lakes, average concentrations are 39.4 $\pm$ 9.3 mg l^{-1} of nitrate, 263 $\pm$ 296 ng l^{-1} of atrazine and 1621 $\pm$ 2099 ng l^{-1} of DEA; in the percolating water, average concentrations are 48.6 $\pm$ 22 mg l^{-1} of nitrate, 2191 $\pm$ 3396 ng l^{-1} of atrazine and 6639 $\pm$ 11 913 ng l^{-1} of DEA (mean and standard deviation are calculated for all the samples of percolating and lake water of the group). Atrazine and DEA have very high concentrations, especially in percolation water, with a maximum for atrazine at Niches of 15 200 ng l^{-1} and a maximum for DEA at Voutes of 52 000 ng l^{-1}. DAR is the highest in this group, especially in the lakes, with a maximum of 42 for Lucarnes and 21 for Voutes. Chloride concentrations are high with a maximum in

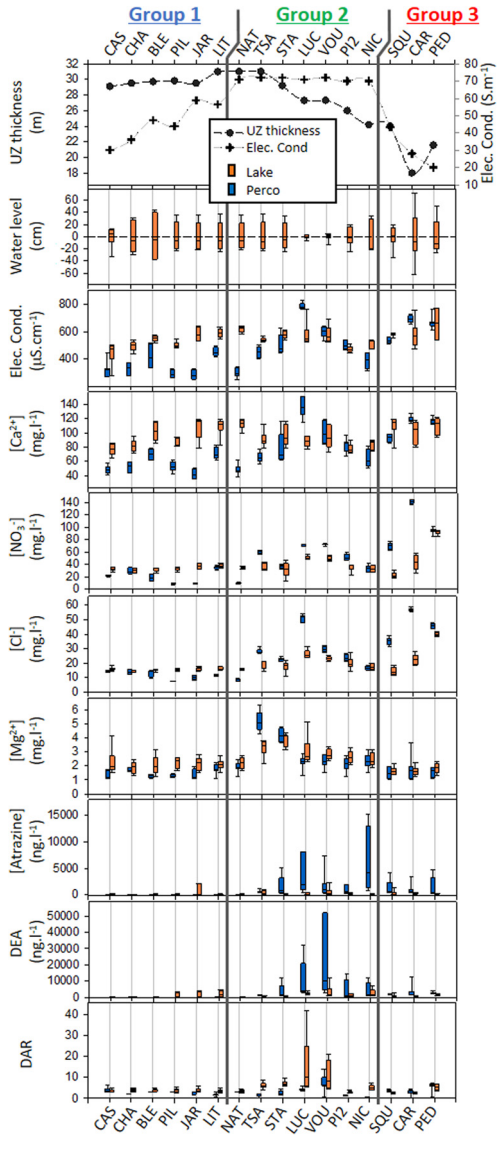

Fig. 4. Hydrodynamic (lake water level) and geochemical analysis of the lakes and the percolating water (electrical conductivity, major ions, pesticides: atrazine and deethylatrazine [DEA], and DAR) for the 16 sites. Box plots for the 12 April, 6 June, 23 June, 5 September 2016 and 9 January, 27 February, 5 September 2017 campaigns.

percolation water of 54 mg l^{-1} for Lucarnes. The highest magnesium concentrations were observed for Group 2 with an average of 2.9 mg l^{-1}.

- *Group 3, the lowest UZ thickness (around 20 m) with a thin layer of CwF*: The water level variation of the lakes is 0.88 m on average. The water of this group is highly contaminated, with higher concentrations in the percolation water. In the lakes, average concentrations are 52.5 $\pm$ 30.9 mg l^{-1} of nitrate, 287 $\pm$ 281 ng l^{-1} of atrazine and 901 $\pm$ 720 ng l^{-1} of DEA; in the percolating water, average concentrations are 105.2 $\pm$ 30.3 mg l^{-1} of nitrate, 1233 $\pm$ 1460 ng l^{-1} of atrazine and 2773 $\pm$ 2534 ng l^{-1} of DEA. The percolation water of Lake Carrefour (the lowest UZ thickness of the 16 sites) has the highest concentrations of nitrate (144 mg l^{-1}) and chloride (59 mg l^{-1}). Pesticide concentrations are rather high with maxima in percolation water of 4800 ng l^{-1} for atrazine in Pedro and 12 800 ng l^{-1} for DEA in Carrefour. In spite of these high concentrations, the DAR is rather constant (around 3) for both the lakes and the percolating water.

Figure 4 also shows the differences in behaviour between nitrate, atrazine and DEA. The size of the boxplots shows the temporal variation for each parameter over the seven campaigns. The standard deviation (SD) calculated for each site, and for each parameter for the seven campaigns gives an indication of this temporal variation. The mean of the SD for all the 16 sites is low for nitrate concentration, 12.3% in lake water and 6.6% in percolating water, while it is high for atrazine and DEA: respectively 91.7% and 79.8% in lake water and 102.3% and 233.6% in percolating water. Thus, the temporal variations are higher for atrazine and DEA than for nitrate. The highest temporal variations are observed for Group 2.

The tritium content in the underground lakes (23 March 2016) and in the percolating water (12 April 2016) are presented in Figure 5. The mean tritium content is 9.2 $\pm$ 1.1 UT in the lakes and 12.1 $\pm$ 1.8 UT in the percolating water. Groundwater sampled in 2016 with concentrations of >10 UT contains a large fraction of water infiltrated in the 1960s.

The lower tritium content in the lakes is evidence that the lake water is composed of younger water than the percolating water. Chen (2019) deduced that the lakes are a mixture of matrix and fissure flow coming from the UZ, while the percolating water is more representative of the matrix water (described in the Discussion).

Temporal approach. The temporal approach is presented for three sites: Bleu, Lucarnes and Pedro, respectively belonging to Groups 1, 2 and 3 with different UZ properties (Figs 2 & 3, Table 1). Firstly, the geochemical and hydrodynamic variations are presented from 2012 to 2020 (Fig. 6) and, secondly, a focus on January 2019 to May 2020 is presented for hydrodynamic data (Fig. 7).

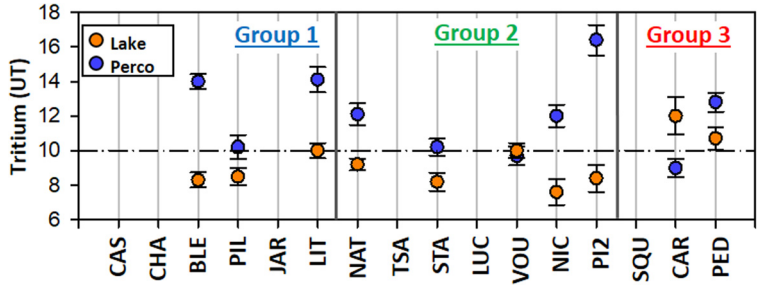

Fig. 5. Tritium concentration in percolating water (12 April 2016) and underground lakes (23 March 2016).

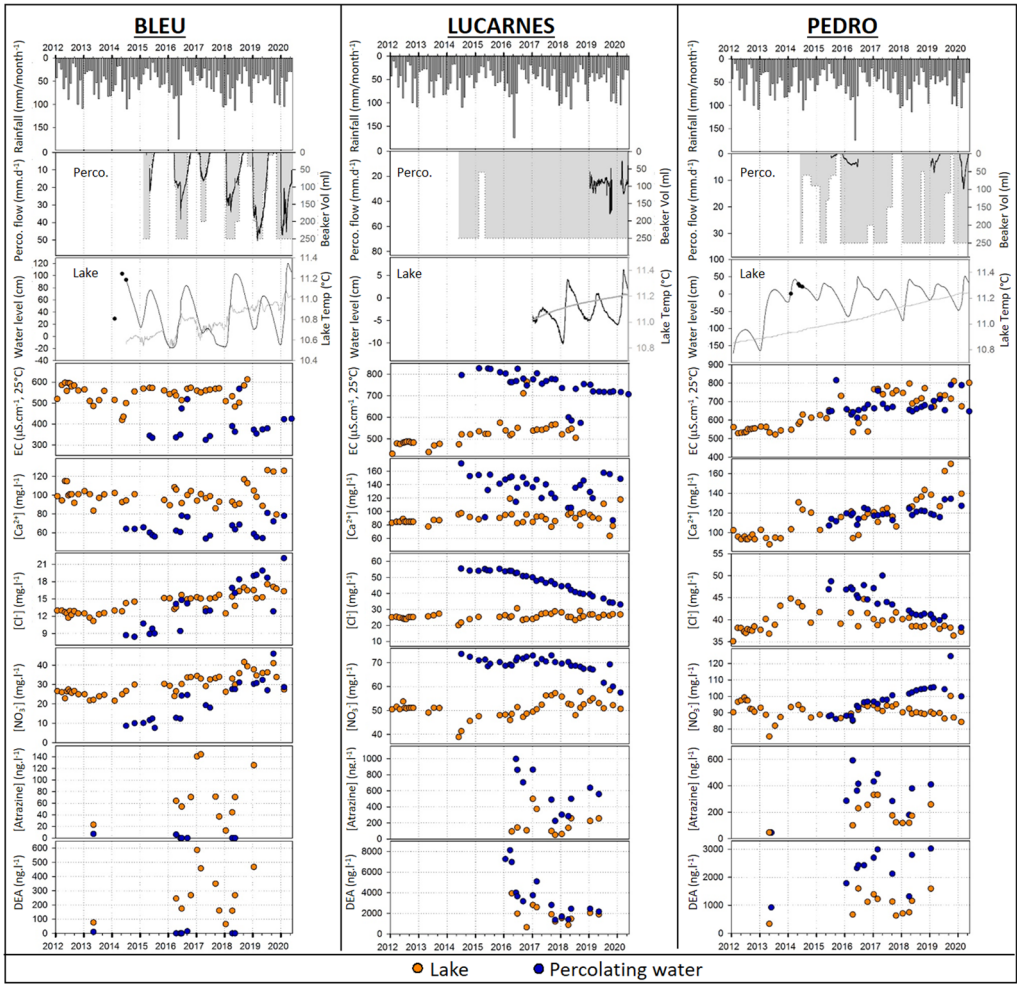

Fig. 6. Time series of rainfall, hydrodynamics, and quality of the percolating water and lakes of the Bleu, Lucarnes and Pedro sites (2012–20). NB: The ranges of the *y*-axes are different from one site to another.

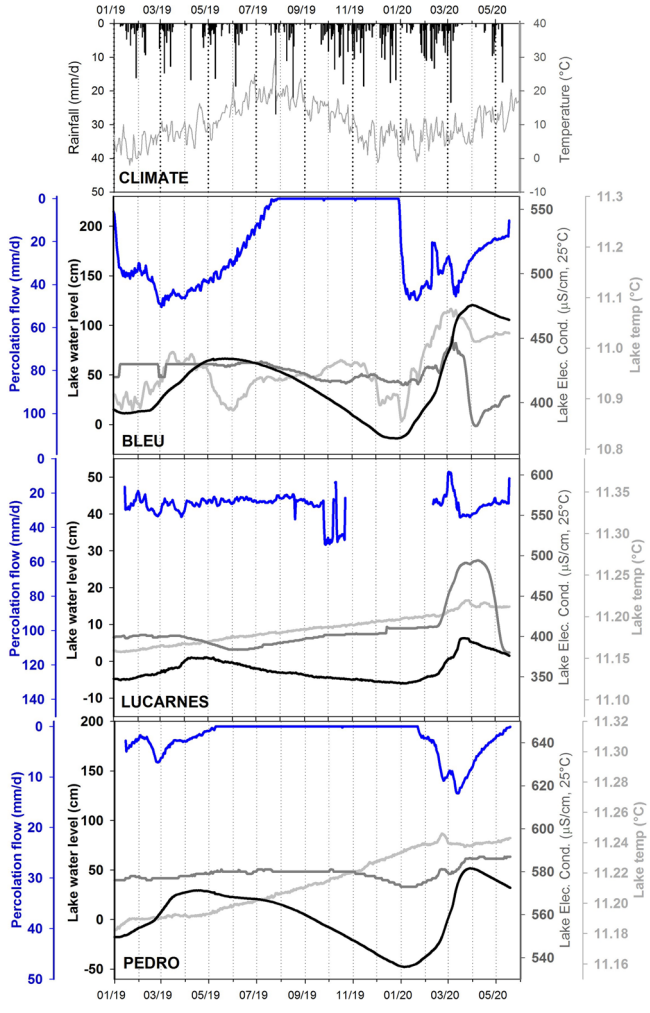

Fig. 7. Climate time series: rainfall and temperature of the outside air. For the groundwater of Bleu, Lucarnes and Voutes: percolation flow, lake water level, temperature and electrical conductivity (1 January 2019–20 May 2020). The *y*-axes are different for each site.

Temporal approach: hydrodynamic and geochemical evolution from 2012 to 2020. Figure 6 shows the rainfall time series at Beauvais station and the hydrodynamic and geochemical variations from 2012 to 2020 for Bleu, Lucarnes and Pedro.

On the Bleu and Pedro sites (Groups 1 and 3 having a thin CwF cover), there is a discontinuity in the percolation season with a shut-off period every year. Percolation starts between January and March and stops between May and August depending on the year. On the Lucarnes site (Group 2 with a thicker CwF cover), percolation is much more continuous. There are small peaks of high-frequency variations in the percolation flow.

The time series of the lake levels correspond with the associated Chalk piezometric variations (data available on ADES database, https://ades.eaufrance.fr), they show annual variations for the three sites, with low levels between December and February and high levels between May and July depending on the site and year. Moreover, the annual lake level amplitude is different on the three sites with an annual variation of about 1 m at Bleu and Pedro (Groups 1 and 3), while it is only about 0.10 m at Lucarnes (Group 2).

The electrical conductivity measurements show seasonal variations of up to 100 µS cm^{-1}. The electrical conductivity of water shows that the ionic content of the groundwater varies between the three sites and that the percolation water and lake water are different: for Bleu, the percolation water is less mineralized than the lake water (perco = 350 µS cm^{-1},

lake = 550 µS cm^{-1}), while for the Lucarnes site, the percolation water is more mineralized than the lake water (perco = 750 µS cm^{-1}, lake = 530 µS cm^{-1}). For Pedro there is very little difference between the two types of water (perco = 680 µS cm^{-1}, lake = 645 µS cm^{-1}). These geochemical differences between lake water and percolation water are found for all major ions as well as for pesticides.

Contamination of quarry groundwater by agricultural input is highly variable, with some water having little contamination (e.g. percolating water at Bleu with $NO_{3\ min}^{-}$ = 10 mg l^{-1} and no trace of pesticide). Some other sites reach extremely high levels of contamination: for example, the percolation water of Lucarnes reaching 1000 ng l^{-1} for atrazine and 5000 ng l^{-1} for DEA, and the lake water and percolation water at the Pedro site with respective nitrate concentrations from 100 to more than 120 mg l^{-1}.

The concentrations of major ions (Fig. 6) show a long-term evolution between 2012 and 2020, but this evolution depends on the type of water (percolation or lake) and on the site.

- For Bleu (Group 1), between 2014 and 2020, the chloride concentration of the lake water increased from about 12 to 17 mg l^{-1}, and for percolation water it increased from 8 to 22 mg l^{-1} between 2016 and 2020; the nitrate concentration also increased from 22 to about 40 mg l^{-1} for the lake water between 2014 and 2020 and from 10 to more than 30 mg l^{-1} for percolation water between 2016 and 2020.
- For Lucarnes (Group 2), the chloride concentration of the lake was stable at around 25 mg l^{-1}, while it decreased in percolation water between 2016 and 2020 (from 55 to 35 mg l^{-1}). The nitrate concentration of the lake was around 50 mg l^{-1}, with a slight tendency to increase, while the concentration in percolation water decreased from around 75 to 55 mg l^{-1} between 2016 and 2020. A slight positive trend toward increase may also be observed in the concentration of calcium in the lake.
- For Pedro (Group 3), between 2016 and 2020, the chloride concentration of the lake was relatively stable at around 40 mg l^{-1}, while it decreased from 45 to 40 mg l^{-1} in percolation water. The nitrate concentration shows a slight decreasing trend around 90 mg l^{-1} for the lake water between 2012 and 2020, while for percolation water it increased from about 85 to 105 mg l^{-1} between 2016 and 2020. Calcium concentration does not show any long-term change, except for Pedro lake water, in which calcium increased from 100 to more than 140 mg l^{-1} between 2012 and 2020.

The seasonal variability of the major ions is rather low. Percolation water does not show any clear seasonal variability. For lakes, there was some seasonal variation in nitrate, chloride and calcium during 2013–14, which seems to be related to the high increase of the lake water level in 2013.

Pesticide concentrations show very high variations in lakes and percolation water. For the Bleu site, the maxima in the lake for atrazine (140 ng l^{-1}) and DEA (600 ng l^{-1}) were observed in January 2017 and the minima for atrazine (20 ng l^{-1}) and DEA (50 ng l^{-1}) were observed in January 2018. The pesticide concentrations in percolation water are below the limit of detection. For the Lucarnes site, lake and percolation water contained pesticides at high concentrations, with the maxima of atrazine and DEA in the lake at 550 and 4000 ng l^{-1}, respectively, while for percolation water it is 1000 ng l^{-1} for atrazine and 8000 ng l^{-1} for DEA. The temporal evolutions of atrazine and DEA concentrations were not correlated, nor do they seem to follow the water level or percolation flow. The Pedro site is also highly contaminated with pesticides, with atrazine maxima of 600 and 350 ng l^{-1} and DEA maxima of 3000 and 1700 ng l^{-1} in percolation and lake water, respectively. For the Pedro site, pesticide concentrations in the percolation water and the lake water appear to be correlated with each other but are not directly related to the lake water level or percolation rate.

The temperature measured in the lakes increased with a trend of about 0.05°C per year. This is consistent with the change in global mean surface temperature (IPCC 2018). If this trend were to remain constant until 2100, global warming by 2100 would be in the order of 5°C. Lake Lucarnes and Lake Pedro do not show any high-frequency variation of temperature, while sub-annual variations were observed for Lake Bleu.

Temporal approach: focus on hydrodynamic evolution from January 2019 to May 2020. The high-frequency time series of hydrodynamic parameters (percolation flow, lake water level), temperature and electrical conductivity of the lakes, for the three sites Bleu, Lucarnes and Pedro, are available between January 2019 and May 2020. Figure 7 shows that the three sites have different behaviours.

For Bleu and Pedro (Groups 1 and 3), the percolation is not permanent. The percolation for Bleu stopped from July 2019 to the end of December 2019, and for Pedro from May 2019 to January 2020. The percolation periods are associated with high lake levels, with an annual variation during 2019–20 of about 1.20 m for Bleu and 0.9 m for Pedro. The time series for Lucarnes (Group 2) showed a permanent percolation that never stopped. The seasonal variation of the lake level (about 0.15 m between January 2020 and April 2020) still showed a slight seasonality.

Variations in temperature and electrical conductivity also show different behaviours between sites (Fig. 7). For Bleu, the electrical conductivity and the lake temperature increased slightly (about 20 µS cm^{-1} and 0.2°C) at the beginning of the recharge, suggesting a piston effect bringing old water. In March 2020, there was a peak in percolation, a higher increase in the lake level, associated with a decrease of about 0.05°C in temperature and a decrease of about 50 µS cm^{-1}in electrical conductivity. This suggests a recharge by relatively recent water. For Lucarnes, the increase in lake level is associated with an increase in conductivity of about 80 µS cm^{-1}, followed by a decrease of more than 120 µS cm^{-1} beginning in April 2020. The temperature shows only an increasing trend without annual or infra-annual variation. For Pedro, electrical conductivity and temperature varied very little, with only a slight increase in electrical conductivity (about 15 µS cm^{-1}) at the beginning of the recharge.

Summary: cross-analysis of groundwater chemical composition and dynamics according to UZ thickness and cover by clay-with-flints

The quarry data are very numerous, 16 sites, two types of water (lake and percolation) per site and, for each of them, many parameters, some constant in time (UZ characteristics), and others variable over time (geochemistry, hydrodynamic parameters).

A good way to summarize all these data is to perform a principal component analysis (PCA) of the 16 lakes and the 16 percolation waters for the seven campaigns of 2016–17. This is a multivariate statistical technique used for the reduction of large datasets. This method is commonly used for environmental studies with a high degree of temporal (Ben Othman *et al.* 1997; Eisenlohr *et al.* 1997) or spatial variation (Wang *et al.* 2001; Valdes *et al.* 2007, 2014).

Data processing: index of hydrodynamic variation of lakes and percolation water. Data processing is necessary as a first step in order to get a homogenized dataset that can be used for PCA, the variations in lake level and percolation flow are indexed, and the I_{hydro} parameter is proposed for comparing the hydrodynamic variations of the lakes and the percolation water. It consists of mean-centring and reduces the percolating flow and lake water level data as shown below for the dataset 'April 2016–September 2017':

$$\text{for percolation: } I_{hydro} = \frac{Q_{perco} - \overline{Q_{perco}}}{SD(Q_{perco})}$$

with Q_{perco} the percolating flow, $\overline{Q_{perco}}$ and SD (Q_{perco}) the mean and standard deviation, respectively, of the percolating flow (calculated on 97 samples from the 16 sites);

$$\text{for the lakes: } I_{hydro} = \frac{H_{lake} - \overline{H_{lake}}}{SD(H_{lake})}$$

with H_{lake} the lake water level, $\overline{H_{lake}}$ and SD (H_{lake}) the mean and the standard deviation, respectively, of the lake level (calculated on 94 samples from the 16 sites).

Principal component analysis. PCA was performed on the UZ characteristics and spatiotemporal data of the groundwater: lake water and percolation water of the 16 sites (dataset 'April 2016–September 2017', presented in Fig. 4).

The PCA was performed on 191 individual samples (94 samples of lake water and 97 samples of percolation water) with 11 active parameters: groundwater electrical conductivity, concentrations of major ions (K^+, Na^+, Ca^{2+}, Mg^{2+}, Cl^-, SO_4^{2-}, NO_3^-), pesticides (atrazine and DEA) and I_{hydro}, and three supplementary parameters: DAR, UZ thickness and CwF thickness.

The structure of the PCA space is strong with three principal components explaining 63.5% of the total variance (Fig. 8). The factor loadings for PC1, PC2 and PC3 are presented in Table 3 and the PC1–PC2 and PC1–PC3 spaces in Figure 9.

Principal Component 1: PC1 (36.5% of the variance) is positively and strongly correlated with electrical conductivity, and the concentrations of Ca^{2+}, Cl^-, SO_4^{2-} and NO_3^-, positively but more weakly correlated with the concentrations of pesticides, and negatively correlated with UZ thickness. The good correlation between Cl^-, SO_4^{2-} and NO_3^- is a common observation in Chalk groundwater (Valdes *et al.* 2006, 2014): Cl^- and SO_4^{2-} are often used in fertilizers, along with NO_3^-. The good correlation with Ca could be explained (1) by the increase in carbonate dissolution associated with nitrate inputs or (2) by the farmer's use of fertilizers that combine

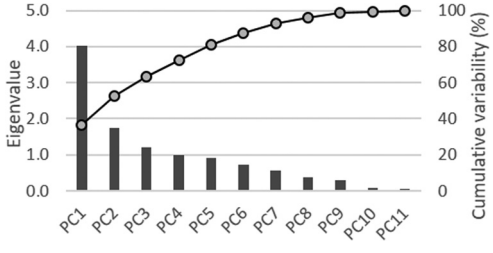

Fig. 8. Eigenvalues and cumulative variability for the 11 principal components (PC) of the PCA.

Table 3. *Factor loadings (%) for the principal components PC1, PC2 and PC3 of the PCA*

	PC1	PC2	PC3
Elec. cond. (µS cm^{-1})	17.67	2.55	3.41
[Ca] (mg l^{-1})	15.45	1.31	4.15
[K] (mg l^{-1})	0.32	38.41	1.04
[Na] (mg l^{-1})	3.77	9.98	18.24
[Mg] (mg l^{-1})	0.03	40.78	9.15
[NO_3] (mg l^{-1})	19.46	0.32	0.07
[Cl] (mg l^{-1})	21.28	0.39	0.24
[SO_4] (mg l^{-1})	13.63	0.00	6.53
[Atrazine] (ng l^{-1})	2.59	0.91	39.49
[DEA] (ng l^{-1})	4.07	0.65	16.51
I_{hydro}	1.74	4.70	1.19

calcium and nitrate. PC1 may be interpreted as a contamination factor, i.e. in the quarry, the thicker the UZ, the less contaminated the groundwater and, inversely, the thinner the UZ, the more contaminated the groundwater.

Principal Component 2: PC2 (15.9% of the variance) is positively and strongly correlated with the concentrations of K^+ and Mg^{2+}, positively but more weakly correlated with CwF thickness, and negatively but weakly correlated with I_{hydro}. Laignel *et al.* (1999), Barhoum *et al.* (2014), and Valdes *et al.* (2014) showed that K^+ and Mg^{2+} can be brought to the Chalk groundwater by the CwF layer, as these clays are mainly composed of smectite, which can contain Na^+, K^+ and Mg^{2+} (Deconinck *et al.* 2005). PC2 may be interpreted as the effect of the CwF thickness on the groundwater: the thicker the CwF layer, the higher the concentrations of Mg^{2+} and K^+ and the lower the hydrodynamic variations (e.g. low variation in lake level and percolation rate).

Principal Component 3: PC3 (11.1% of the variance) is positively and strongly correlated with the concentration of atrazine and DEA, especially due to values measured in the percolation of Group 2. CwF thickness and Mg also contribute positively but more weakly. PC3 may be interpreted as the contamination by the axis of pesticides. Even if the variance of this axis is low (11.1%), PC3 gives evidence of the relationship between the CwF thickness and the pesticide concentration: the higher the CwF thickness, the higher the pesticide contamination.

The individuals are plotted in the PC1–PC2 and PC1–PC3 spaces (Fig. 9). The distribution of the individuals is consistent with the three groups: Group 1 is in the negative part of PC1 (low contamination) and has low PC2 values (low impact of the CwF); Group 3 is globally in the positive part of PC1 (high contamination) and has low PC2 values (low impact of the CwF); Group 2 is very dispersed in the PC1–PC2 space. The range of contamination is substantial (samples from not contaminated to highly contaminated) and some samples are highly impacted by CwF. The PC1–PC3 space distinguishes the percolating water of Group 2 from other types of water that are heavily contaminated with atrazine and DEA.

The surface inputs of the UZ are (1) rainwater, which is homogeneous at the surface above the quarry, (2) chemical elements from Chalk dissolution or clay–water interaction and (3) anthropogenic inputs used for agriculture, which are considered to be homogeneous on the fields above the quarry (slight differences exist in the quantity of atrazine and nitrate from one field to another). The differences in the quality and hydrodynamics of the groundwater observed in the three groups show that the transfer processes differ depending on the properties of the UZ, among which are the CwF thickness and the UZ thickness. The role of these two parameters will be discussed in the following section.

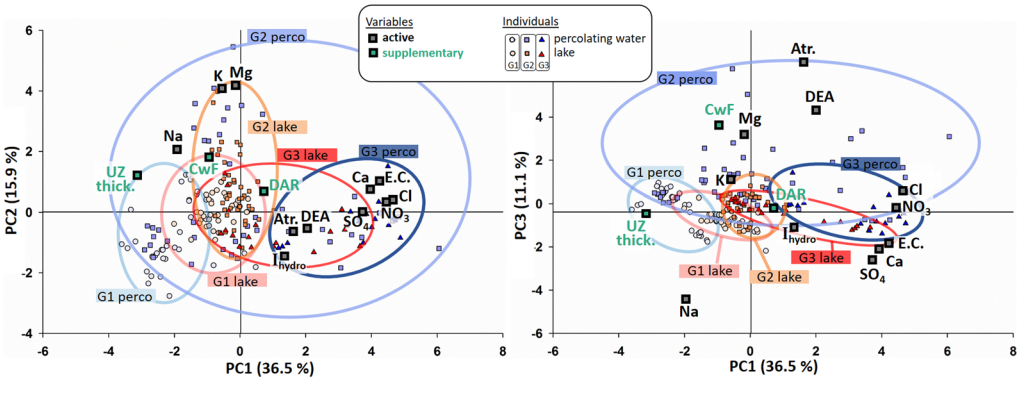

Fig. 9. PCA of the groundwater and UZ properties. PC1–PC2 and PC1–PC3 spaces with variables and individuals. The lakes are represented in red and the percolation waters in blue.

In Figure 9, the distribution of lake water differs from that of percolating water: the lakes of the three groups are centred in the middle of the factorial space, whereas the percolation water is more scattered. The scattering of individuals representing the percolation water is greater than that of lake individuals.

Discussion

The underground quarry of Saint-Martin-le-Nœud allows for the investigation of the chemical composition and dynamics of groundwater over a small area of the Chalk aquifer (0.18 km^2) in the Paris Basin. The differences observed between the various sites and between lake water and percolating water are surprising if we consider the size of the quarry. The variations may be interpreted in terms of differences in the transfer processes. They also show that the proportion of water flowing through fractures or the matrix may differ.

Transfer through matrix and fractures

The Chalk of the study area is described as a double-porosity medium with fractures and a matrix (Barhoum *et al.* 2014). Many studies have focused on the transfer processes, but the proportion of water in the fractures to that in the matrix, as well as the related velocities, remains difficult to assess. Most studies consider that recharge occurs mainly through the matrix (Mathias *et al.* 2005; Cooper *et al.* 2006; Ireson and Butler 2011). Smith *et al.* (1970) estimated that transfer through the matrix accounts for 70–85% of the total recharge. Some authors consider that transfer through fractures only occurs under specific conditions, such as high rainfall events and high soil moisture (Haria *et al.* 2003; Ireson and Butler 2011). Other studies observed that flow occurs mainly through fractures in the winter (Keim *et al.* 2012).

Rapid responses of the water table to rain events are often observed in the Chalk aquifer, which can result from a direct transfer from the surface (infiltration and transfer of rain water from the surface to the water table through the fractures), but also from a 'piston effect' mechanism: in this case, the water stored in the matrix of the UZ of Chalk is pushed by pressure and goes down slowly without mixing with overlying recent water (Downing *et al.* 2005; Ireson *et al.* 2006).

Water velocity in the Chalk matrix using percolating water. This section is mainly based on the paper by Chen *et al.* (2019*a*), who estimated the age of the percolation water in the Saint-Martin-le-Nœud quarry, thus allowing for the estimation of the transfer velocities in the Chalk UZ based on nitrate, atrazine and tritium (Figs 4 & 5) as dating tracers. Tritium is an inherent constituent of the water molecule, and thus its transfer time corresponds to that of water. Nitrate and atrazine are dissolved molecules, and thus their transfer may be different from that of water, especially for atrazine, which may be delayed by sorption (Coquet 2003). For nitrate and even more for atrazine, the transfer time would be greater than the transfer time of water.

Transfer time was estimated as follows: in oxidizing conditions, the absence of nitrate contamination provides evidence of water infiltrated before 1950. Tritium content up to 10 UT gives evidence of water infiltrated in the 1960s and the presence of atrazine or metabolite demonstrates water infiltrated between 1977 and 2003. Transfer velocities were computed for each environmental tracer (nitrate, atrazine and tritium) by dividing the estimated transfer time by the depth of each site.

The water collected at the ceiling of the quarry, at the base of the UZ: about 1–2 m above the water table, has a residence time of roughly a few decades. A summary of the results for the three groups is given in Table 4. The estimated tritium/water velocities range from 0.37 to over 0.72 m a^{-1}. The three tracers have velocities that may differ from each other, demonstrating that there is actually a mixture of water with different velocities. The results are slightly different for the three groups, with the maximum velocity for Group 2. The transfer velocities are then higher for a thicker CwF layer.

These results of vertical velocity of water in the UZ may be used to estimate the hydraulic conductivity of the matrix.

$$V = \frac{K\,i}{n_e} \rightarrow K = \frac{V\,n_e}{i}$$

with K the hydraulic conductivity, i the hydraulic gradient and n_e the effective porosity.

The vertical hydraulic gradient (i) may be estimated at 1, as the pore space is almost all filled by water held by the narrow pore throats. The effective

Table 4. *Range of velocities for the three groups deduced from tracers: tritium content, atrazine and nitrate concentrations in the percolation water*

	Range of velocity(m a^{-1})		
	With tritium	**With atrazine**	**With nitrate**
Group1	0.51 ± 0.03–0.73 ± 0.4	$<0.76 \pm 0.15$	$<0.45 \pm 0.02$
Group2	0.48 ± 0.02–0.70 ± 0.04	0.72 ± 0.14–2.15 ± 0.43	$>0.45 \pm 0.02$
Group3	0.37 ± 0.02–0.53 ± 0.03	0.54 ± 0.11–1.63 ± 0.33	$>0.32 \pm 0.02$

From Chen *et al.* (2019*a*).

porosity n_e is around 0.4. According to Chen *et al.* (2019*a*), a range of velocities from 0.1 to 1 m a^{-1} is chosen for the calculation. The calculated hydraulic conductivity ranges from 1.3×10^{-9} to 1.1×10^{-8} m s^{-1}. These values of hydraulic conductivity clearly correspond to the matrix hydraulic conductivity and are consistent with the literature (Megnien 1978; Price 1987; Bloomfield 1996).

Mixing of water from matrix and fractures in lakes. The lake water is a mixture of percolating water (visible at the quarry ceiling) and water flowing in the unsaturated Chalk through the walls and the pillars of the quarry (not visible). Even if the spatial variation of the water quality between the lakes shows the same trend as the percolating water, the lake water has a quality different from the associated percolating water (Figs 4–6 & 9). The water flowing through the pillars and walls of the quarry is therefore not only composed of matrix water, but also of fracture water that is recent water.

Two geochemical arguments allow us to assume that the lake water is younger than the percolating water sampled from the roof above the lake.

- For the lakes in Group 1, there is little contamination in the percolation while some lakes are slightly more contaminated with nitrate or atrazine (Fig. 4), showing the contribution of more recent water.
- The tritium content is lower in the lakes than in the percolating water (mean, 9.2 $\pm$ 1.1 UT in the lakes; mean, 12.1 $\pm$ 1.8 UT in the percolating water, Fig. 5), giving evidence of a proportion of fracture flow.

The hydrodynamic time series (water level, electrical conductivity and temperature of the lakes, Figs 6 & 7) provide information on the transfer processes. Chen (2019) estimated the time responses as 106–157 days, using cross-correlations between water level and effective rainfall. Considering the UZ thickness above each lake, she deduced velocities from 58 to 83 m a^{-1}. These values correspond to velocities currently observed in the fractures.

The time series of the lake water level combined with those of temperature and electrical conductivity values (Fig. 7) are helpful to determine whether this velocity corresponds to direct transfer or to a piston effect.

The temperature variation of Lake Bleu gives evidence of direct transfer from the surface, meaning a contribution of recent water flowing throughout the fractures. For Lake Lucarnes and Lake Pedro, the temperature variation is lower: The contribution of recent water from direct transfer is probably lower for these sites.

For the three sites – Bleu, Lucarnes and Pedro – the electrical conductivity value increases as the water level increases, giving evidence of a piston effect process: more mineralized water is brought to the lake corresponding to old water pushed with pressure. Nevertheless, a large decrease in electrical conductivity was observed in March 2020 for Lake Bleu at the moment of maximum recharge, indicating surface water infiltration. A small decrease was also observed in Lake Pedro at the end of February 2020, showing that direct transfer contributed a small proportion of water. These direct and rapid transfers, even if they seem to contribute only little to the recharge, are proof of fracture flow at the sites.

To summarize, the water table is mainly composed of 'old' water resulting from transfer through the matrix at a velocity of about 1 m a^{-1}, but with a small contribution of rapid transfer through the fractures at an average velocity of approximately 60–80 m a^{-1}.

Contaminant transport and degradation

The concentrations of agricultural contaminants are very high in groundwater (with the maxima of nitrate concentration at 144 mg l^{-1}, atrazine at 15 200 ng l^{-1} and DEA at 52 000 ng l^{-1}; Table 2) compared to regional studies on Chalk groundwater. For NO_3^-, El Gaouzi *et al.* (2013) observed concentrations between 34 and 49 mg l^{-1} in boreholes or springs in the Paris Basin. Sorensen *et al.* (2015) found nitrate concentrations ranging from 30 to 60 mg l^{-1} for the Chalk aquifer in the UK. For pesticides, Baran *et al.* (2008) observed concentrations of atrazine between 50 and 100 ng l^{-1} and of DEA between 100 and 200 ng l^{-1} in the Paris Basin from 2000 to 2006. In the Chalk aquifer in Belgium, Hakoun *et al.* (2017) measured the highest concentrations of atrazine and DEA at less than 200 ng l^{-1}.

At Saint-Martin-le-Nœud, the concentrations of nitrate, atrazine and DEA vary spatially along the quarry both in lakes and percolating water. According to PCA (Fig. 9), the first factor explaining these variations is UZ thickness. The higher the UZ thickness, the lower the contaminant concentrations.

Figure 10 presents the nitrate concentration from 2014 to 2019 in the percolation water at different depths (=UZ thickness). It highlights the nitrate profile with a nitrate peak at about 15–20 m deep. The nitrate peak descends slowly with a rate of 0.3 to 0.5 m a^{-1} (Chen *et al.* 2019*a*) depending on the site. Concentrations have increased for most points, and sometimes intensely (e.g. nitrate concentration at Bleu increased by more than 30 mg l^{-1} in 5 years, Figs 6 & 10). For these sites, the concentrations will probably continue to increase, as shown in Figure 6, until they reach the peak over 140 mg l^{-1}. Only two sites show a different evolution: Carrefour is the most superficial of all the

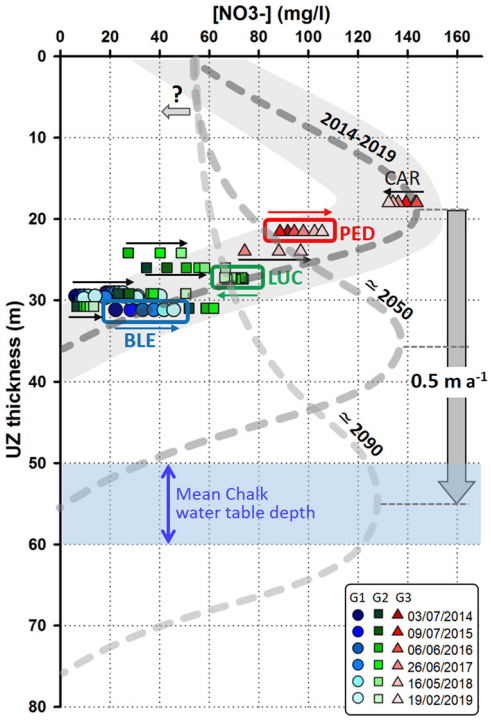

Fig. 10. Nitrate profile in the UZ. Nitrate concentrations in the percolation waters from 2014 to 2019 for the 16 sites for the different UZ thicknesses. BLE, Bleu; LUC, Lucarnes; PED, Pedro; CAR, Carrefour; and future profiles in 2050 and 2090 with a transfer velocity of nitrate in the UZ of 0.5 m s^{-1}.

sites with only 18 m of UZ; the percolating water is therefore younger. The peak of nitrate probably occurred around or before 2014. The Lucarnes UZ thickness is substantial (27 m) but has the highest transfer velocity in the UZ. Therefore, the nitrate peak has probably already been reached here as well. In the future, the nitrate peak will continue to go down. With a very simple approach, considering a velocity of 0.5 m a^{-1}, the peak could reach a depth of about 35 m in 2050. The water table in the Paris Basin is approximately 50–60 m deep and, in this context, the nitrate peak could reach the water table around 2090. This approach is raw since diffusion phenomena are not taken into account. Moreover, a single velocity is considered, whereas it would be necessary to take into account the heterogeneity of the transfer velocities according to the properties of the UZ. Nevertheless, a strong increase in nitrate concentrations in groundwater can clearly be expected in the coming decades. The very high levels of contamination observed in the quarry can be explained by the configuration of the site. The percolation and lake water come exclusively from the agricultural area and the water is taken from the upper groundwater table without dilution. This high level of agricultural contamination is rarely observed in boreholes and springs. However, it can be assumed that the concentrations found in the UZ matrix (from percolation) are representative of the storage of contaminants in the Chalk UZ in agricultural areas.

The transfer and the degradation of atrazine residues through the Chalk aquifer UZ in Saint-Martin-le-Nœud has already been published in Chen *et al.* (2019*b*). A summary of the results is presented here, supplemented by additional observations on percolation.

Firstly, atrazine transfer velocities from the soil surface toward the water table were estimated (Table 4) to be in the range of 0.54–2.15 m a^{-1} (Chen *et al.* 2019*a*).

Secondly, the spatial variations of atrazine and DEA concentrations are very high for both lake and percolation water and are related to the spatial variations of UZ thickness and the thickness of the CwF layer, as follows:

(1) For the UZ thickness, in the case of Saint-Martin-le-Nœud at present, the deepest groundwater is globally less contaminated. More generally, the transfer time is directly related to the depth of the water table: the deeper the groundwater, the older the water.

(2) For the thickness of the CwF layer, the relationship with pesticide concentrations is more complex. In our case, the third principal component PC3 of the PCA (Table 3, Fig. 9) shows a correlation between the CwF thickness and the pesticide concentration: the higher the CwF thickness, the higher the atrazine contamination. Furthermore, this type of agricultural soil is favourable for growing maize where atrazine was used. The UZ thickness of Group 1 is quite similar to that of Group 2, whereas the thickness of CwF is higher in Group 2. The concentration of pesticide is very low for Group 1, whereas it is very high and variable for Group 2. Chen *et al.* (2019*a*, *b*) deduced that the transfer velocities are the highest under a thick layer of CwF. Moreover, Chen *et al.* (2019*b*) showed that the degradation processes (expressed by the DAR) are the greatest for a thick CwF layer. The degradation of atrazine is a biological process, occurring mainly in the soil (Johnson *et al.* 2000). Chen *et al.* (2019*b*) hypothesize that the CwF layer allows for the formation of a 'perched water table', leading to atrazine staying near the surface for extended periods of time, resulting in the degradation processes. The role of the CwF layer in transfer processes is detailed in the next section.

The behaviour of atrazine and DEA is different from that of nitrate (Figs 4, 6 & 9). Firstly, the periods of application are different (nitrate after the 1950s and atrazine from 1977 to 2003); secondly, atrazine is applied once a year in April whereas nitrate can be applied several times a year. However, examination of the time series (Fig. 6) shows that the temporal variations of these three molecules also differ, especially under a thick CwF layer, demonstrating the differences in the transfer processes. Chen *et al.* (2019*b*) showed that transfers of atrazine and DEA are shifted in connection with their sorption characteristics.

The role of the CwF layer on Chalk groundwater

In karst Chalk of Upper Normandy (France), Jardani *et al.* (2006) and Valdes *et al.* (2014) studied the CwF layer. Firstly, Jardani *et al.* (2006) observed a perched water table at the surface, particularly in CwF layers, and they also showed that this layer is heterogeneous with preferential pathways. Secondly, Valdes *et al.* (2014) showed that more preferential pathways exist under a thick CwF layer. They used the map of turbidity in Chalk groundwater to provide a rough estimation of the degree of connection of the water table to the surface and they compared it with the map of CwF thickness. A good correlation shows the more karstic areas (i.e. a higher degree of connection between the surface and water table) correspond to the higher CwF thickness. This can be explained by the process of CwF formation: the CwF results from the weathering of Chalk (Laignel *et al.* 1999), and thus a thick layer of CwF indicates that a significant amount of Chalk dissolution has occurred allowing for the presence of larger karst conducts or larger fractures. To summarize, Valdes *et al.* (2014) established that a thick CwF layer allows for storage of perched groundwater in the UZ in which biogeochemical processes can occur, followed by a delayed and concentrated infiltration via preferential pathways. The exact location of this water storage is difficult to define. Jardani *et al.* (2006) observed water storage and water movement in the CwF (allowed by CwF heterogeneities), but also in the overlying loess at their study site.

The Chalk of Saint-Martin-le-Nœud is clearly less karstified than the Chalk of Upper Normandy, but similar transfer processes may be advanced. The results presented here show that in the case of a thick CwF layer:

(1) Infiltrated water is stored in the near surface, forming a sort of 'near-surface perched groundwater', that could be located in the CwF layer and in the covering soil. This is supported by the following arguments:
   - The farmer indicates that he cannot sow wheat on this plot (root rot due to the high water content of the soil).
   - The greatest pesticide degradation processes measured in the area with thick CwF indicate a long residence time near the surface.
   - The permanent percolation flow and the low variation in the lake level may be explained by the storage of water in a 'near-surface perched groundwater', which will continuously and slowly discharge into the Chalk UZ.

(2) The infiltration may be concentrated. This is supported by the previous arguments and the geometry of the CwF (Fig. 3) that shows the presence of depressions that could facilitate

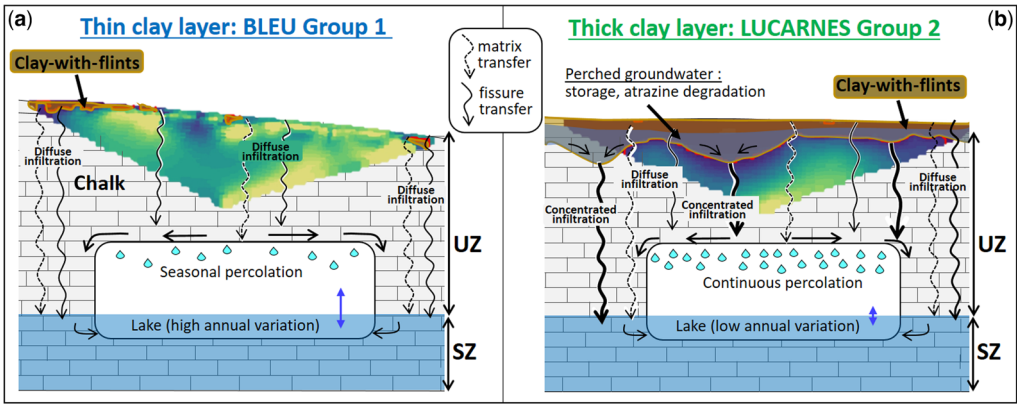

Fig. 11. Sketches of transfer processes through the Chalk UZ with the geophysical profiles of ERT (**a**) with thin clay-with-flints illustrated by the Bleu site and (**b**) with thick clay-with-flints illustrated by the Lucarnes site.

concentrated infiltration with potential preferential pathways, as described by Jardani *et al.* (2006).

(3) The transfer velocity in the UZ is higher. This is supported by the velocities deduced from the environmental tracers nitrate, atrazine and tritium, which are highest under a thick CwF in our study site.

Figure 11 presents two sketches of transfer processes through the Chalk UZ with a thin CwF layer and a thick CwF layer. In the case of a thin layer of CwF (Fig. 11a, Bleu site), there is no perched water table and the degradation processes are lower. The infiltration is diffuse and the recharge is seasonal, with high variations in percolation flow (percolation only during part of the year) and in the lake water level. In the case of a thick layer of CwF (Fig. 11b, Lucarnes site), a perched water table is formed in the CwF, allowing for degradation of the atrazine. The geometry of the CwF with depressions indicates that preferential pathways are located at the bottom of these depressions. The infiltration of water is delayed and concentrated, enabling a continuous recharge throughout the year, inducing low variability in the percolation flow and in the lake water level. The transfer velocities of contaminants are higher and the transfer of atrazine and DEA are different because of the desorption processes.

Conclusions

The Saint-Martin-le-Nœud underground quarry is a unique site for the study of water and contaminant transfers in the Chalk aquifer. Firstly, it gives access to both the UZ at different depths and the SZ (the water table) directly. Secondly, the UZ characteristics are spatially variable at the scale of the quarry, which allows improved understanding of the role of the UZ thickness and CwF layer in the geochemical and hydrodynamic behaviour of groundwater. Thirdly, the detailed monitoring from 2012 onwards allows study of the longer-term evolution of the Chalk groundwater.

This study provides new insights into the following points presented in the introduction

(1) *The local variability in groundwater behaviours upon reaching the water table*

Chalk groundwater has highly variable hydrodynamic behaviour and geochemical properties, although the measuring points are very close to each other. The groundwater, here supplied exclusively by the UZ, may have little contamination, or very high concentrations of nitrate and atrazine, over small spatial scales.

(2) *The balance of fracture v. matrix flow*

The Chalk groundwater is mostly old (a few decades in this study) and, therefore, water transfer processes occur mainly in the matrix. At Saint-Martin-le-Nœud, the estimated water velocities in the Chalk matrix range from 0.37 to over 0.72 m a^{-1} and the estimated hydraulic conductivity ranges from 1.3×10^{-9} to 1.1×10^{-8} m s^{-1}. However, a small part of recent water flowing through the fractures is highlighted. The proportion of water flow between the matrix and fractures remains difficult to determine, although this question may be addressed thanks to a detailed analysis of the hydrodynamic chronicles (time series) and the addition of other dating tracers.

(3) *The transport of contaminants*

The percolating water has shown storage of agricultural contaminants in the Chalk UZ, which percolates slowly toward the water table through the matrix via the piston effect, at speeds similar to the water velocity or below. It can be assumed that the deep groundwater, today not contaminated, will have a large increase in nitrate, atrazine and DEA concentrations in the future and for many years. Moreover, other contaminants used later, such as other pesticides (metolachlor, acetochlor, dimethenamid, etc.), pharmaceutical products (antibiotics, hormones, etc.), or other industrial contaminants are probably stored today in the Chalk UZ and will likely reach the Chalk water table in the future.

(4) *The role of the CwF cover on the water and contaminant transfer in the Chalk aquifer*

The CwF layer, often considered protective in the past, plays a role in the hydrodynamics and the quality of the groundwater. This layer allows a perched water table to be created near the surface, which makes the degradation processes of pesticides possible. This perched water table then flows to the unsaturated Chalk by more concentrated infiltration through preferential pathways with higher transfer velocity and continuous recharge throughout the year. This mainly explains the high variations of pesticide concentrations for a thick CwF layer. Furthermore, the DAR results demonstrate that degradation processes occur where CwF is thick.

The acquisition of such a multidisciplinary dataset on the Saint-Martin-le-Nœud quarry is a very important work, both in the field (on the surface or underground) and in the laboratory; but the results show the importance of long-term *in situ* measurements for a better understanding of the water and contaminant transfer processes in the Chalk.

Acknowledgements The authors thank the SNO Karst (CNRS) for the integration of the project into their research network. They also thank the Conservatoire d'Espaces Naturels de Picardie for access to the quarry. The authors would like to thank the reviewers and the Editor for their helpful comments.

Competing interests The authors declare that they have no known competing financial interests or personal relationships that could have appeared to influence the work reported in this paper.

Author contributions **DV**: conceptualization (lead), data curation (equal), funding acquisition (lead), investigation (equal), methodology (lead), project administration (lead), supervision (lead), writing – original draft (lead), writing – review & editing (lead); **NC**: data curation (equal), formal analysis (equal), investigation (lead), validation (equal); **MD**: data curation (supporting), investigation (equal), methodology (supporting); **CM**: conceptualization (equal), methodology (equal); **HB**: data curation (equal), methodology (equal), validation (equal); **RG**: data curation (supporting), methodology (supporting), supervision (supporting); **JG**: methodology (supporting); **FA**: data curation (equal), formal analysis (equal); **RN**: data curation (equal), investigation (equal); **EA**: data curation (equal); **MR**: data curation (supporting), formal analysis (supporting), investigation (supporting); **CF**: data curation (equal); **PG**: conceptualization (supporting); **PR**: conceptualization (supporting), supervision (supporting).

Funding The authors gratefully acknowledge funding provided to DV by IPSL (ID0E6UBI3597, ID0EZFCI3599), Conseil Régional, Île-de-France (ID0EM4BI3598) and CNRS (EC2CO).

Data availability All data generated or analysed during this study are included in this published article (and its supplementary information files)

References

AESN 2020. Contamination des cours d'eau et des eaux souterraines du bassin seine-Normandie par les pesticides et leurs produits de dégradation: Etat des lieux 2019. https://fr.calameo.com/agence-de-l-eau-seine-normandie/read/004001913aa51314580c6

Ascott, M.J., Wang, L., Stuart, M.E., Ward, R.S. and Hart, A. 2016. Quantification of nitrate storage in the vadose (unsaturated) zone: a missing component of terrestrial N budgets. *Hydrological Processes*, **30**, 1903–1915, https://doi.org/10.1002/hyp.10748

Baran, N., Lepiller, M. and Mouvet, C. 2008. Agricultural diffuse pollution in a chalk aquifer (Trois Fontaines, France): influence of pesticide properties and hydrodynamic constraints. *Journal of Hydrology*, **358**, 56–69, https://doi.org/10.1016/j.jhydrol.2008.05.031

Barhoum, S. 2014. *Transferts dans la craie: approche régionale: le Nord-Ouest du Bassin de Paris: approche locale: la carrière de Saint-Martin-le-Nœud*. PhD thesis, Université Pierre et Marie Curie – Paris VI, France.

Barhoum, S., Valdes, D., Guerin, R., Marlin, C., Vitale, Q., Benmamar, J. and Gombert, P. 2014. Spatial heterogeneity of high-resolution Chalk groundwater geochemistry – underground quarry at Saint Martin-le-Nœud, France. *Journal of Hydrology*, **519**, 756–768, https://doi.org/10.1016/j.jhydrol.2014.08.001

Barker, J.A. and Foster, S.S.D. 1981. A diffusion exchange model for solute movement in fissured porous rock. *Quarterly Journal of Engineering Geology and Hydrogeology*, **14**, 17–24, https://doi.org/10.1144/GSL.QJEG.1981.014.01

Ben Othman, D., Luck, J.-M. and Tournoud, M.-G. 1997. Geochemistry and water dynamics: application to short time-scale flood phenomena in a small Mediterranean catchment: I. Alkalis, alkali-earths and Sr isotopes. *Chemical Geology*, **140**, 9–28, https://doi.org/10.1016/S0009-2541(97)00004-1

Blanchoud, H., Alliot, F., Chen, N. and Valdes, D. 2020. Rapid SPE – LC MS/MS analysis for atrazine, its by-products, simazine and S metolachlor in groundwater samples. *Methods X*, **7**, 2020, https://doi.org/10.1016/j.mex.2020.100824

Bloomfield, J. 1996. Characterisation of hydrogeologically significant fracture distributions in the Chalk: an example from the Upper Chalk of southern England. *Journal of Hydrology*, **184**, 355–379, https://doi.org/10.1016/0022-1694(95)02954-0

BRGM 1969. *Carte hydrogéologique de la France à 1/50 000 – Beauvais (HYD014)*. BRGM, Orléans.

Brouyère, S. 2006. Modeling the migration of contaminants through variably saturated dual-porosity, dual-permeability chalk. *Journal of Contaminant Hydrology*, **82**, 195, https://doi.org/10.1016/j.jconhyd.2005.10.004

Brouyère, S., Dassargues, A. and Hallet, V. 2004. Migration of contaminants through the unsaturated zone overlying the Hesbaye chalky aquifer in Belgium: a field investigation. *Journal of Contaminant Hydrology*, **72**, 135e164, https://doi.org/10.1016/j.jconhyd.2003.10.009

Cao, F., Jaunat, J. *et al.* 2020. Heterogeneous behaviour of unconfined Chalk aquifers infer from combination of groundwater residence time, hydrochemistry and hydrodynamic tools. *Journal of Hydrology*, **581**, 124433, https://doi.org/10.1016/j.jhydrol.2019.124433

Chefetz, B., Bilkis, Y.I. and Polubesova, T. 2004. Sorption desorption behavior of triazine and phenylurea herbicides in Kishon river sediments. *Water Research*, **38**, 4383e4394, https://doi.org/10.1016/j.watres.2004.08.023

Chen, N. 2019. *Processus de transferts dans la zone non saturée de la craie (approche in situ et laboratoire)*. PhD thesis, Sorbonne University, Paris, France.

Chen, N., Valdes, D., Marlin, C., Blanchoud, H., Guerin, R., Rouelle, M. and Ribstein, P. 2019*a*. Water, nitrate and atrazine transfer through the unsaturated zone of the Chalk aquifer in northern France. *Science of the Total Environment*, **652**, 927–938, https://doi.org/10.1016/j.scitotenv.2018.10.286

Chen, N., Valdes, D., Marlin, C., Ribstein, P., Alliot, F., Aubry, E. and Blanchoud, H. 2019*b*. Transfer and

degradation of the common pesticide atrazine through the unsaturated zone of the Chalk aquifer (Northern France). *Environmental Pollution*, **255**, 113125, https://doi.org/10.1016/j.envpol.2019.113125

Comly, H.H. 1945. Cyanosis in infants caused by nitrates in well water. *JAMA*, **129**, 112–116, https://doi.org/10.1001/jama.1945.02860360014004

Cooper, J.D., Gardner, C.M.K. and Mackenzie, N. 2006. Soil controls on recharge to aquifers. *European Journal of Soil Science*, **41**, 613e630.

Coquet, Y. 2003. Sorption of pesticides atrazine, isoproturon, and metamitron in the vadose zone. *Vadose Zone Journal*, **2**, 40–51, https://doi.org/10.2113/2.1.40

Daily, W. and Owen, E. 1991. Cross-borehole resistivity tomography. *Geophysics*, **56**, 1228–1235, https://doi.org/10.1190/1.1443142

Deconinck, J.-F., Amédro, F., Baudin, F., Godet, A., Pellenard, P., Robaszynski, F. and Zimmerlin, I. 2005. Late Cretaceous palaeoenvironments expressed by the clay mineralogy of Cenomanian–Campanian chalks from the east of the Paris Basin. *Cretaceous Research*, **26**, 171–179, https://doi.org/10.1016/j.cretres.2004.10.002

Downing, R.A., Price, M. and Jones, G.P. (eds) 2005. *The Hydrogeology of the Chalk of North-West Europe*. Oxford University Press, Oxford.

Edmunds, W.M., Shand, P., Hart, P. and Ward, R.S. 2003. The natural (baseline) quality of groundwater: a UK pilot study. *Science of the Total Environment*, **310**, 25–35, https://doi.org/10.1016/S0048-9697(02)00620-4

Eisenlohr, L., Bouzelboudjen, M., Kiraly, L. and Rossier, Y. 1997. Numerical versus statistical modeling of natural response of a karst hydrogeological system. *Journal of Hydrology*, **202**, 244–262, https://doi.org/10.1016/S0022-1694(97)00069-3

El Gaouzi, F.Z.J., Sebilo, M. *et al*. 2013. Using $\delta^{15}N$ and $\delta^{18}O$ values to identify sources of nitrate in karstic springs in the Paris basin France. *Applied Geochemistry*, **35**, 230e243, https://doi.org/10.1016/j.apgeochem.2013.04.015

Espejo-Herrera, N., Gràcia-Lavedan, E. *et al*. 2016. Colorectal cancer risk and nitrate exposure through drinking water and diet. *International Journal of Cancer*, **139**, 334–346, https://doi.org/10.1002/ijc.30083

Foster, S.S.D., Cripps, A.C. and Smith-Carington, A. 1982. Nitrate leaching to groundwater. *Philosophical Transactions of the Royal Society B*, **296**, 477–489, https://doi.org/10.1098/rstb.1982.0021

Gaillardet, J., Braud, I. *et al*. 2018. OZCAR: the French network of critical zone observatories. *Vadose Zone Journal*, **17**, 180067, https://doi.org/10.2136/vzj2018.04.0067

Gillon, M., Crançon, P. and Aupiais, J. 2010. Modelling the baseline geochemistry of groundwater in a Chalk aquifer considering solid solutions for carbonate phases. *Applied Geochemistry*, **25**, 1564–1574, https://doi.org/10.1016/j.apgeochem.2010.08.006

Griffiths, D.H. and Barker, R.D. 1993. Two-dimensional resistivity imaging and modelling in areas of complex geology. *Journal of Applied Geophysics*, **29**, 211–226, https://doi.org/10.1016/0926-9851(93)90005-J

Gutierrez, A. and Baran, N. 2009. Long-term transfer of diffuse pollution at catchment scale: respective roles of soil, and the unsaturated and saturated zones (Brévilles, France). *Journal of Hydrology*, **369**, 381–391, https://doi.org/10.1016/j.jhydrol.2009.02.050

Hakoun, V., Orban, P., Dassargues, A. and Brouyère, S. 2017. Factors controlling spatial and temporal patterns of multiple pesticide compounds in groundwater (Hesbaye chalk aquifer, Belgium). *Environmental Pollution*, **223**, 185–199, https://doi.org/10.1016/j.envpol.2017.01.012

Haria, A.H., Hodnett, M.G. and Johnson, A.C. 2003. Mechanisms of groundwater recharge and pesticide penetration to a chalk aquifer in southern England. *Journal of Hydrology*, **275**, 122–137, https://doi.org/10.1016/S0022-1694(03)00017-9

INERIS 2010. Impact du changement climatique sur la stabilité des cavités souterraines: Bilan des données de l'année 2009. Rapport d'étude, DRS-10- 95052-00919A.

IPCC 2018. Global warming of 1.5°C. *In*: Masson-Delmotte, V., Zhai, P. *et al*. (eds) *An IPCC Special Report on the Impacts of Global Warming of 1.5°C above Pre-Industrial Levels and Related Global Greenhouse Gas Emission Pathways, in the Context of Strengthening the Global Response to the Threat of Climate Change, Sustainable Development, and Efforts to Eradicate Poverty*.

Ireson, A.M. and Butler, A.P. 2011. Controls on preferential recharge to Chalk aquifers. *Journal of Hydrology*, **398**, 109e123, https://doi.org/10.1016/j.jhydrol.2010.12.015

Ireson, A.M., Wheater, H.S., Butler, A.P., Mathias, S.A., Finch, J. and Cooper, J.D. 2006. Hydrological processes in the Chalk unsaturated zone – insights from an intensive field monitoring programme. *Journal of Hydrology*, **330**, 29–43, https://doi.org/10.1016/j.jhydrol.2006.04.021

Ireson, A.M., Mathias, S.A., Wheater, H.S., Butler, A.P. and Finch, J. 2009. A model for flow in the chalk unsaturated zone incorporating progressive weathering. *Journal of Hydrology*, **365**, 244, https://doi.org/10.1016/j.jhydrol.2008.11.043

Issa, S. and Wood, M. 1999. Degradation of atrazine and isoproturon in the unsaturated zone: a study from Southern England. *Pesticide Science*, **55**, 539e545, https://doi.org/10.1002/(SICI)1096-9063(199905)55:5<539::AID-PS970>3.0.CO;2-8

Jardani, A., Dupont, J.P. and Revil, A. 2006. Self-potential signals associated with preferential groundwater flow pathways in sinkholes. *Journal of Geophysical Research*, **111**, B09204, https://doi.org/10.1029/2005JB004231

Johnson, A.C., White, C. and Lal Bhardwaj, C. 2000. Potential for isoproturon, atrazine and mecoprop to be degraded within a chalk aquifer system. *Journal of Contaminant Hydrology*, **44**, 1e18, https://doi.org/10.1016/S0169-7722(00)00092-9

Jourde, H., Massei, N. *et al*. . 2018. SNO KARST: a French network of observatories for the multidisciplinary study of critical zone processes in karst watersheds and aquifers. *Vadose Zone Journal*, **17**, https://doi.org/10.2136/vzj2018.04.0094

Keim, D.M., West, L.J. and Odling, N.E. 2012. Convergent flow in unsaturated fractured chalk. *Vadose Zone Journal*, **11**, vzj2011.0146, https://doi.org/10.2136/vzj2011.0146

Klinck, B., Hopson, P. *et al*. 1998. *The hydrogeological behaviour of the clay-with-flints of southern England*. British Geological Survey Technical Report **WE/97/5**.

Kloppmann, W., Dever, L. and Edmonds, W.M. 1994. Isotopic and geochemical investigations of Chalk groundwater of the Champagne region, France. *Zeitschrift der Deutschen Geologischen Gesellschaft*, **145**, 143–152, https://doi.org/10.1127/zdgg/145/1994/143

Kloppmann, W., Dever, L. and Edmunds, W.M. 1998. Residence time of Chalk groundwaters in the Paris Basin and the North German Basin: a geochemical approach. *Applied Geochemistry*, **13**, 593–606, https://doi.org/10.1016/S0883-2927(97)00110-8

Lafrance, N. 2016. *Etude des effets de l'eau sur les phénomènes de rupture et de déformation affectant les carrières souterraines de craie*. PhD thesis, Université de Lorraine, France.

Laignel, B., Quesnel, F., Meyer, R. and Bourdillon, C. 1999. Reconstruction of the upper cretaceous chalks removed by dissolution during the Cenozoic in the western Paris Basin. *International Journal of Earth Sciences*, **88**, 467e474, https://doi.org/10.1007/s005310050279

Lallahem, S. 2002. *Structure et modélisation hydrodynamique des eaux souterraines: application à l'aquifère crayeux de la bordure nord du Bassin de Paris*. PhD thesis, Université Lille 1, France.

Lapworth, D.J., Baran, N., Stuart, M.E., Manamsa, K. and Talbot, J. 2015. Persistent and emerging micro-organic contaminants in Chalk groundwater of England and France. *Environmental Pollution*, **203**, 214e225, https://doi.org/10.1016/j.envpol.2015.02.030

Le Noë, J.L., Billen, G., Esculier, F. and Garnier, J. 2017. Long-term socioecological trajectories of agro-food systems revealed by N and P flows in French regions from 1852 to 2014. *Agriculture, Ecosystems & Environment*, **265**, 132–143, https://doi.org/10.1016/j.agee.2018.06.006

Maloszewski, P. and Zuber, A. 1996. Lumped parameter models for the interpretation of environmental tracer data. *Manual on Mathematical Models in Isotope Hydrogeology. TECDOC-910*. International Atomic Energy Agency, Vienna, Austria, 9–58.

Mathias, S.A., Butler, A.P., McIntyre, N. and Wheater, H.S. 2005. The significance of flow in the matrix of the Chalk unsaturated zone. *Journal of Hydrology*, **310**, 62e77, https://doi.org/10.1016/j.jhydrol.2004.12.009

McNeill, J.D. 1980. *Electromagnetic terrain conductivity measurement at low induction numbers*. Technical Note TN-6, Geonics Limited.

Megnien, C. 1978. *Hydrogéologie du centre du bassin de Paris: Contribution à l'étude de quelques aquiferes principaux*. PhD thesis, Université Pierre et Marie Curie, France.

Orban, P., Brouyère, S. *et al*. 2010. Regional transport modelling for nitrate trend assessment and forecasting in a chalk aquifer. *Journal of Contaminant Hydrology*, **118**, 79–93, https://doi.org/10.1016/j.jconhyd.2010.08.008

Price, M. 1987. Fluid flow in the Chalk of England. *Geological Society, London, Special Publications*, **34**, 141–156, https://doi.org/10.1144/GSL.SP.1987.034.01.1

Smith, D.B., Wearn, P.L., Richards, H.J. and Rowe, P.C. 1970. Water movement in the unsaturated zone of high and low permeability strata by measuring natural tritium. *Isotope Hydrology 1970*. Symposium on Use of Isotopes in Hydrology, Vienna, Austria, 9–13 March 1970. International Atomic Energy Agency, Vienne, 73–86.

Smith, J.T., Clarke, R.T. and Bowes, M.J. 2010. Are groundwater nitrate concentrations reaching a turning point in some chalk aquifers? *Science of the Total Environment*, **408**, 4722–4732, https://doi.org/10.1016/j.scitotenv.2010.07.001

Sorensen, J.P.R., Butcher, A.S., Stuart, M.E. and Townsend, B.R. 2015. Nitrate fluctuations at the water table: implications for recharge processes and solute transport in the Chalk aquifer. *Hydrological Processes*, **29**, 3355e3367, https://doi.org/10.1002/hyp.10447

Stuart, M.E. and Smedley, P.L. 2009. *Baseline Groundwater Chemistry: the Chalk Aquifer of Hampshire (Open report No. OR/09/052)*. British Geological Survey.

Surdyk, N., Gourcy, L., Bault, V. and Baran, N. 2021. Nitrate transport in the chalk vadose zone in Picardy, France. *Geological Society, London, Special Publications*, **517**, https://doi.org/10.1144/SP517-2020-164

Thatcher, L.L., Janzer, V.J. and Edwards, K.W. 1977. *Methods for Determination of Radioactive Substances in Water and Fluvial Sediments (USGS numbered series no. 05-A5). Techniques of Water-Resources Investigations*. US Government Printing Office.

Valdes, D., Dupont, J.-P., Massei, N., Laignel, B. and Rodet, J. 2005. Analysis of karst hydrodynamics through comparison of dissolved and suspended solids' transport. *Comptes Rendus Geoscience*, **337**, 1365–1374, https://doi.org/10.1016/j.crte.2005.07.011

Valdes, D., Dupont, J.-P., Massei, N., Laignel, B.T. and Rodet, J. 2006. Investigation of karst hydrodynamics and organization using autocorrelations and T-[Delta]C curves. *Journal of Hydrology*, **329**, 432–443, https://doi.org/10.1016/j.jhydrol.2006.02.030

Valdes, D., Dupont, J.-P., Laignel, B., Ogier, S., Leboulanger, T. and Mahler, B.J. 2007. A spatial analysis of structural controls on karst groundwater geochemistry at a regional scale. *Journal of Hydrology*, **340**, 244–255, https://doi.org/10.1016/j.jhydrol.2007.04.014

Valdes, D., Dupont, J.-P., Laignel, B., Slimani, S. and Delbart, C. 2014. Infiltration processes in karstic chalk investigated through a spatial analysis of the geochemical properties of the groundwater: the effect of the superficial layer of clay-with-flints. *Journal of Hydrology*, **519**, 23–33, https://doi.org/10.1016/j.jhydrol.2014.07.002

Wang, L., Stuart, M.E. *et al*. 2012. Prediction of the arrival of peak nitrate concentrations at the water table at the regional scale in Great Britain. *Hydrological Processes*, **26**, 226–239, https://doi.org/10.1002/hyp.8164

Wang, Y., Ma, T. and Luo, Z. 2001. Geostatistical and geochemical analysis of surface water leakage into groundwater on a regional scale: a case study in the Liulin karst system, northwestern China. *Journal of Hydrology*, **246**, 223–234, https://doi.org/10.1016/S0022-1694(01)00376-6